

On Adaptive Transmission for Distributed Detection in Energy Harvesting Wireless Sensor Networks with Limited Fusion Center Feedback

Ghazaleh Ardeshiri, Azadeh Vosoughi *Senior Member, IEEE*

Abstract—We consider a wireless sensor network, consisting of N heterogeneous sensors and a fusion center (FC), tasked with solving a binary distributed detection problem. Sensors communicate directly with the FC over orthogonal fading channels. Each sensor can harvest randomly arriving energy and store it in a battery. Also, it knows its quantized channel state information (CSI), acquired via a limited feedback channel from the FC. We propose a transmit power control strategy such that the J -divergence based detection metric is maximized, subject to an average transmit power per sensor constraint. The proposed strategy is parametrized in terms of the channel gain quantization thresholds and the scale factors corresponding to the quantization intervals, to strike a balance between the rates of energy harvesting and energy consumption for data transmission. This strategy allows each sensor to adapt its transmit power based on its battery state and its quantized CSI. Finding the optimal strategy requires solving a non-convex optimization problem that is not differentiable with respect to the optimization variables. We propose near-optimal strategy based on hybrid search methods that have a low-computational complexity.

Index Terms—power control, distributed detection, channel gain quantization, energy harvesting, J -divergence.

I. INTRODUCTION

In a conventional wireless sensor network (WSN), sensors powered by non-rechargeable batteries are used to sense and collect data for various applications. The energy constraint imposed by the non-rechargeable batteries has inspired a rich body of research on developing signal processing and transmission strategies to achieve balance between network lifetime and performance. Recently, the technology of harnessing energy from the renewable resources of energy in ambient environment has attracted attention of many researchers, as a promising solution to address the challenging energy constraint problem in WSNs. In particular, energy harvesting (EH)-powered sensors offer potential for transforming design and performance of WSNs tasked with detection or estimation of a signal source [3]. In practice, the energy arrival of ambient energy sources is intrinsically time-variant and often sporadic. To flatten the randomness of the energy arrival, the harvested energy is stored in a battery, to balance the energy arrival and the energy consumption. Power/energy management in EH-enabled WSNs with finite size batteries is necessary, in order to balance the rates of energy harvesting and energy consumption for transmission. If the energy management policy is overly aggressive, sensors may stop functioning, due

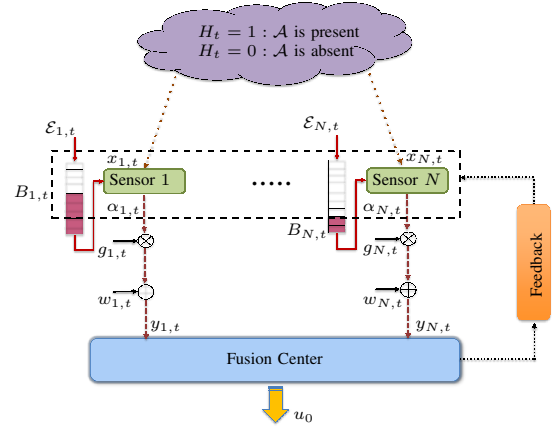


Fig. 1: Our system model and the schematic of battery state in time slot t .

to energy outage. On the other hand, if the policy is overly conservative, sensors may fail to utilize the excess energy, due to energy overflow, leading into a performance degradation.

In this work, we adopt a WSN model that consists of several distributed sensors and a fusion center (FC). The FC is tasked with solving a binary-hypothesis distributed detection problem. Each sensor is capable of harvesting energy from the ambient environment and is equipped with a battery of finite size to store the harvested energy. Sensors process locally their observations and communicate directly with the FC over orthogonal fading channels¹. Each sensor only knows the quantized channel state information (CSI), via a limited feedback channel from the FC, and adapts its transmit power according to its battery state and its quantized CSI. The FC jointly processes the received signals and makes a global decision about the underlying hypotheses (see Fig. 1). In the following we provide a concise review of the literature that are most related to our work.

A. Related Works and Knowledge Gap

The classical problem of binary distributed detection in a network has a long and rich history [4], [5]. Motivated by the potential applications of WSNs for event detection, researchers have expanded these classical studies to include the effects of wireless communication channels between the sensors and the FC on the local decision rules at the sensors and the

Parts of this work were presented in GlobalSIP 2018 [1] and GLOBECOM 2019 [2].

¹The orthogonal channels are assigned using frequency-division duplexing.

fusion rule at the FC [6]–[8]. To reduce energy consumption, researchers have further explored optimal power control strategies [9], [10] that allow sensors to adapt their transmit powers based on the states of their propagation channels and the local sensor statistics. In particular, the authors in [9], [10] have designed the optimal power control strategies that maximize a J -divergence based detection metric for binary-hypothesis and multiple-hypothesis distributed detection problems, respectively. We note that [9], [10] assume that the CSI is perfectly available at the sensors for power control. However, CSI acquisition at the sensors in WSNs is difficult. In time division duplexing systems, sensors need to perform training-based channel estimation to acquire CSI [11]–[13]. In frequency division duplexing systems, sensors can acquire quantized CSI via a limited feedback channel from the FC [14]. We note that signal adaptation at the sensors according to the quantized CSI received from a limited feedback channel has been considered before for data communications [15] and distributed estimation of a signal source [16], [17].

It is worth pointing out that, while the studies in [9]–[14] on optimal power control strategies can be applied to WSNs with conventional battery-powered sensors, they cannot be applied to EH-enabled WSNs. None of these works have considered the new challenges related to power/energy management imposed by the random nature of the energy arrival and the harvested energy.

In the context of distributed detection, there are only few studies that consider EH-powered sensors [18]–[20], among which [18] is the closest work to ours. Modeling the battery state as a two-state Markov chain and choosing Bhattacharya distance as the detection performance metric, the authors in [18] have investigated the optimal local decision thresholds at the sensors, such that the detection performance is optimized. Considering an EH-powered node, that is deployed to monitor the change in its environment, the authors in [19] formulated a quickest change detection problem, where the goal is to detect the time at which the underlying distribution of sensor observation changes. Choosing error probability as the detection performance metric, the authors in [20] proposed ordered transmission schemes, that can lead to a smaller average number of transmitting sensors, without comprising the detection performance. None of the works in [18]–[20] have addressed transmit power control problem. Energy harvesting has been also considered in the contexts of cooperative data communication [21], [22], distributed estimation of a signal source [23], [24], and cognitive radio systems [25], [26].

To the best of our knowledge, adaptive (channel-dependent) power control strategies in an EH-enabled WSN, where sensors can adapt their transmit powers based on their quantized CSI, with the goal of optimizing a detection metric, have not been explored. Hence, this is the focus of our work.

B. Our Contribution

Given our adopted WSN model (see Fig. 1), we aim at developing a transmit power control strategy for sensors that strikes a balance between energy harvesting and energy consumption for data transmission, and optimizes the

detection performance. We choose the J -divergence between the distributions of the detection statistics at the FC under two hypotheses, as the detection performance metric. Our choice is motivated by the facts that (i) it is a widely used metric for evaluating detection performance [9], [10], [13], [14], since it provides a lower bound on the detection error probability. Indeed, maximizing the J -divergence is equivalent to minimizing the lower bound on the error probability; (ii) it allows us to provide a more tractable analysis. Our proposed power control strategy is parametrized in terms of the channel gain quantization thresholds and the scale factors (corresponding to the quantization intervals). The scale factors play key roles in balancing the rates of energy harvesting and energy consumption for transmission. We seek the jointly optimal scale factors and the quantization thresholds such that the J -divergence at the FC is maximized, subject to an average transmit power per sensor constraint. This optimization problem can be solved *offline* at the FC, given the statistical information of fading channels and the energy arrival. The solutions to this optimization problem is available *a priori* at the sensors, such that each sensor can adapt its transmit power according to its battery state and its quantized CSI that is received from the FC via the feedback channel. Our main contributions can be summarized as follow:

- Our system model encompasses the stochastic energy arrival model for harvesting energy, and the stochastic energy storage model for the finite-size battery. We model the randomly arriving energy units during a time slot as a Poisson process, and the dynamics of the battery as a finite state Markov chain.
- We propose a novel parametrized power control strategy and formulate problem (P1) to optimize the parameters such that the J -divergence at the FC is maximized, subject to an average transmit power per sensor constraint.
- We derive an approximate expression for the detection error probability, relying on Lindeberg Central Limit Theorem (CLT) for large number of sensors.
- Since (P1) is not concave with respect to the optimization variables, and the objective function and the constraints in (P1) are not differentiable with respect to these variables, we resort to grid-based search methods. In particular, we consider deterministic, random, and hybrid search methods, and explore the trade-offs in their performance and computational complexity. We show that the proposed hybrid search methods have the lowest computational complexity and provide a close-to-optimal performance.
- We show that the optimized transmit power level is not a monotonic function of the channel gain (given the battery state), and explore the trade-off between transmit power and detection performance.

C. Paper Organization

The paper organization follows: Section II describes our system and observation models and introduces our constrained optimization problem (P1). Section III derives a closed-form expression for the total J -divergence and an approximate expression for the error probability corresponding to the optimal

Bayesian fusion rule at the FC. Sections IV and V formulate and solve problem (P1), respectively. Section VI illustrates our numerical results. Section VII concludes our work.

II. SYSTEM MODEL

A. Observation Model at Sensors

To describe our signal processing blocks at sensors and the FC as well as energy harvesting model, we divide time horizon into slots of equal length T_s . Each time slot is indexed by an integer t for $t = 1, 2, \dots, \infty$. We model the underlying binary hypothesis H_t in time slot t as a binary random variable $H_t \in \{0, 1\}$ with a-priori probabilities $\Pi_0 = \Pr(H_t = 0)$ and $\Pi_1 = \Pr(H_t = 1) = 1 - \Pi_0$. We assume that the hypothesis H_t varies over time slots in an independent and identically distributed (i.i.d.) manner. Let $x_{n,t}$ denote the local observation at sensor n in time slot t . We assume that sensors' observations given each hypothesis with conditional distribution $f(x_{n,t}|H_t = h_t)$ for $h_t \in \{0, 1\}$ are independent across sensors. This model is relevant for WSNs that are tasked with detection of a known signal in uncorrelated Gaussian noises with the following signal model

$$\begin{aligned} H_t = 1 : x_{n,t} &= \mathcal{A} + v_{n,t}, \\ H_t = 0 : x_{n,t} &= v_{n,t}, \quad \text{for } n = 1, \dots, N, \end{aligned} \quad (1)$$

where Gaussian observation noises $v_{n,t} \sim \mathcal{N}(0, \sigma_{v_n}^2)$ are independent over time slots and across sensors. Given observation $x_{n,t}$ sensor n forms local log-likelihood ratio (LLR)

$$\Gamma_n(x_{n,t}) \triangleq \log \left(\frac{f(x_{n,t}|h_t = 1)}{f(x_{n,t}|h_t = 0)} \right), \quad (2)$$

and uses its value to choose its non-negative transmission symbol $\alpha_{n,t}$ to be sent to the FC. In particular, when LLR is below a given local threshold θ_n , sensor n does not transmit and let $\alpha_{n,t} = 0$. When LLR exceeds the given local threshold θ_n , sensor n chooses $\alpha_{n,t}$ according to its battery state and the feedback information about its communication channel. Choice of $\alpha_{n,t}$ will be explained later in Section II-B.

B. Battery State, Harvesting and Transmission Models

We assume sensors are equipped with identical batteries of finite size K cells (units), where each cell corresponds to b_u Joules of stored energy. Therefore, each battery is capable of storing at most Kb_u Joules of harvested energy. Let $B_{n,t} \in \{0, 1, \dots, K\}$ denote the discrete random process indicating the battery state of sensor n at the beginning slot t . Note that $B_{n,t} = 0$ and $B_{n,t} = K$ represent the empty battery and full battery levels, respectively. Also, $B_{n,t} = k$ implies that the battery is at state k , i.e., k cells of the battery is charged and the amount of stored energy in the battery is kb_u Joules.

Let $\mathcal{E}_{n,t}$ denote the randomly arriving energy units² during time slot t at sensor n . We assume $\mathcal{E}_{n,t}$'s are i.i.d. over time slots and across sensors. We model $\mathcal{E}_{n,t}$ as a Poisson random variable with parameter ρ , and probability mass function (pmf) $p_e \triangleq \Pr(\mathcal{E}_{n,t} = e) = e^{-\rho} \rho^e / e!$ for $e = 0, 1, \dots, \infty$. Note that parameter ρ is the average number of arriving energy units

during one time slot at each sensor. Let $\mathcal{S}_{n,t}$ be the number of stored (harvested) energy units in the battery at sensor n during time slot t . Note that the harvested energy $\mathcal{S}_{n,t}$ cannot be used during slot t . Since the battery has a finite capacity of K cells, we have $\mathcal{S}_{n,t} \in \{0, 1, \dots, K\}$. Also, $\mathcal{S}_{n,t}$ are i.i.d. over time slots and across sensors. We can find the pmf of $\mathcal{S}_{n,t}$ in terms of the pmf of $\mathcal{E}_{n,t}$. Let $q_e \triangleq \Pr(\mathcal{S}_{n,t} = e)$ for $e = 0, 1, \dots, K$. We have³

$$q_e = \begin{cases} p_e, & \text{if } 0 \leq e \leq K-1, \\ \sum_{m=K}^{\infty} p_m, & \text{if } e = K. \end{cases} \quad (3)$$

Let $g_{n,t}$ indicate the fading channel gain between sensor n and the FC during time slot t . We assume block fading model and $g_{n,t}$'s are i.i.d. over time slots and independent across sensors. We assume there is a limited feedback channel from the FC to the sensors [14], through which sensor n is informed of the quantization interval to which $g_{n,t}$ belongs. In particular, suppose the positive real line is partitioned into L disjoint intervals $\mathcal{I}_{n,l} = [\mu_{n,l}, \mu_{n,l+1})$ for $l = 0, \dots, L-1$, using the quantization thresholds $\{\mu_{n,l}\}_{l=0}^L$, where $0 = \mu_{n,0} < \mu_{n,1} < \dots < \mu_{n,L} = \infty$ (to be optimized). The quantization mapping rule follows: if the quantizer input $g_{n,t}$ lies in the interval $\mathcal{I}_{n,l}$ then the quantizer output is $\mu_{n,l}$. Let $\pi_{n,l} = \Pr(g_{n,t} \in \mathcal{I}_{n,l})$ be the probability that $g_{n,t}$ lies in the interval $\mathcal{I}_{n,l}$. This probability depends on the distribution of fading model. For instance, for Rayleigh fading model $g_{n,t}^2$ has exponential distribution with the mean $\mathbb{E}\{g_{n,t}^2\} = \gamma_{g_n}$ and we have

$$\pi_{n,l} = \Pr \left(g_{n,t}^2 \in [\mu_{n,l}^2, \mu_{n,l+1}^2) \right) = e^{-\frac{\mu_{n,l}^2}{\gamma_{g_n}}} - e^{-\frac{\mu_{n,l+1}^2}{\gamma_{g_n}}}. \quad (4)$$

Let $\mathcal{P}_{n,t}$ denote the transmit power of sensor n in time slot t . When LLR is below a given local threshold θ_n , sensor n does not transmit, i.e., $\mathcal{P}_{n,t} = 0$. When LLR exceeds θ_n , sensor n chooses $\mathcal{P}_{n,t}$ according to its battery state k and the feedback information. In particular, we choose a transmit power control strategy where $\mathcal{P}_{n,t}$ is proportional to the amount of stored energy in the battery, i.e., kb_u Joules, and the scale factor depends on the feedback information. Mathematically, we express $\mathcal{P}_{n,t}$ as the following

$$\mathcal{P}_{n,t} = \begin{cases} 0, & \Gamma_n(x_{n,t}) < \theta_n, \\ \lfloor c_{n,0} k \rfloor b_u / T_s, & \Gamma_n(x_{n,t}) \geq \theta_n, g_{n,t} \in \mathcal{I}_{n,0}, \\ \vdots & \vdots \\ \lfloor c_{n,L-1} k \rfloor b_u / T_s, & \Gamma_n(x_{n,t}) \geq \theta_n, g_{n,t} \in \mathcal{I}_{n,L-1}, \end{cases} \quad (5)$$

where $\lfloor \cdot \rfloor$ is the floor function and the scale factors $\{c_{n,l}\}_{l=0}^{L-1}$ are between zero and one. The number of scale factors is equal to the number of quantization levels and scale factor $c_{n,l}$ corresponds to the quantization interval $\mathcal{I}_{n,l} = [\mu_{n,l}, \mu_{n,l+1})$. Given θ_n , the problem of optimizing transmit power control strategy reduces to finding the best scale factors $\{c_{n,l}\}_{l=0}^{L-1}$ and

³Equation (3) assumes that the energy storage process is lossless. For a lossy storage process, one needs to model such loss via establishing a functional relationship between $\mathcal{S}_{n,t}$ and $\mathcal{E}_{n,t}$, i.e., $\mathcal{S}_{n,t} = f_n(\mathcal{E}_{n,t})$, where the function $f_n(\cdot)$ can be approximated using the battery type and specifications. Knowing $f_n(\cdot)$ and the pmf of $\mathcal{E}_{n,t}$, one can find the pmf of $\mathcal{S}_{n,t}$ using transformation method.

²Suppose each arriving energy unit measured in Joules is b_u Joules.

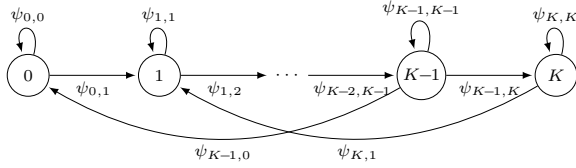


Fig. 2: Schematics of Markov chain corresponding to the battery state random process $B_{n,t}$.

the quantization thresholds $\{\mu_{n,l}\}_{l=1}^{L-1}$ such that a specified performance metric is optimized. We let the transmit symbol $\alpha_{n,t} = \sqrt{\mathcal{P}_{n,t}}$. Considering the power control strategy in (5), we note that the number of energy units consumed for transmitting symbol $\alpha_{n,t}$ is $\lfloor c_{n,l}k \rfloor$, which is an integer between zero and K and is always smaller than k . In other words, the energy consumption for transmission cannot exceed the stored energy in the battery, and the battery cannot be fully depleted after a transmission. It also implies that when $\lfloor c_{n,l}k \rfloor = 0$ the sensor will not transmit. Note that the scale factors $\{c_{n,l}\}_{l=0}^{L-1}$ in (5) play key roles in balancing the rates of energy harvesting and energy consumption for transmission. Given the quantization thresholds $\mu_{n,l}$'s, when $c_{n,l}$'s are closer to one, such that the rate of energy consumption for transmission is greater than the rate of energy harvesting, sensors may stop functioning, due to energy outage. When $c_{n,l}$'s are closer to zero, such that the rate of energy consumption for transmission is smaller than the rate of energy harvesting, sensors may fail to utilize the excess energy, due to energy overflow, leading into a performance degradation.

The battery state at the beginning of slot $t+1$ depends on the battery state at the beginning of slot t , the harvested energy during slot t , and the number of stored energy units that is consumed for transmitting symbol $\alpha_{n,t}$, i.e., $\mathcal{P}_{n,t}T_s/b_u$. Mathematically, we express $B_{n,t+1}$ as the following

$$B_{n,t+1} = \min \{ [B_{n,t} + \mathcal{S}_{n,t} - \mathcal{P}_{n,t}T_s/b_u]^+, K \}, \quad (6)$$

where $[x]^+ = \max\{0, x\}$. Considering the dynamic battery state model in (6) we note that, conditioned on $\mathcal{S}_{n,t}$ and $\mathcal{P}_{n,t}$ the value of $B_{n,t+1}$ only depends on the value of $B_{n,t}$ (and not the battery states of time slots before t). Hence, the process $B_{n,t}$ can be modeled as a Markov chain. Fig. 2 is the schematic representation of this $(K+1)$ -state Markov chain. Let $\Phi_{n,t}$ be the probability vector of battery state in slot t

$$\Phi_{n,t} \triangleq [\Pr(B_{n,t} = 0), \dots, \Pr(B_{n,t} = K)]^T, \quad (7)$$

where the superscript T indicates transposition. We note that $\Pr(B_{n,t} = k)$ in (7) depends on $B_{n,t-1}$, $\mathcal{S}_{n,t-1}$ and $\mathcal{P}_{n,t-1}$. Assuming that the Markov chain is time-homogeneous⁴, we let Ψ_n be the corresponding $(K+1) \times (K+1)$ transition probability matrix of this chain with its (i,j) -th entry $\psi_{i,j} \triangleq \Pr(B_{n,t} = j | B_{n,t-1} = i)$ for $i, j = 0, \dots, K$. Defining the indicator function $I_{i \rightarrow j}(\mathcal{S}_{n,t}, \mathcal{P}_{n,t}T_s/b_u)$ as (8). We can express $\psi_{i,j}$ as below

$$\begin{aligned} \psi_{i,j} = & \hat{\Pi}_{n,1} \sum_{k=0}^K \sum_{l=0}^L \pi_{n,l} q_k I_{i \rightarrow j}(\mathcal{S}_{n,t}, \lfloor c_{n,l}i \rfloor) \\ & + \hat{\Pi}_{n,0} \sum_{k=0}^K q_k I_{i \rightarrow j}(\mathcal{S}_{n,t}, 0). \end{aligned} \quad (9)$$

The symbols $\hat{\Pi}_{n,0}$ and $\hat{\Pi}_{n,1}$ in (9) refer to the probabilities of events $\mathcal{P}_{n,t} = 0$ and $\mathcal{P}_{n,t} \neq 0$, respectively. In particular, we have

$$\begin{aligned} \hat{\Pi}_{n,0} &= \Pr(\mathcal{P}_{n,t} = 0) = \Pi_0(1 - P_{f_n}) + \Pi_1(1 - P_{d_n}), \\ \hat{\Pi}_{n,1} &= \Pr(\mathcal{P}_{n,t} \neq 0) = \Pi_0 P_{f_n} + \Pi_1 P_{d_n}, \end{aligned} \quad (10)$$

where the probabilities P_{f_n} and P_{d_n} can be determined using our signal model in (1)

$$\begin{aligned} P_{f_n} &= \Pr(\mathcal{P}_{n,t} \neq 0 | h_t = 0) = Q\left(\frac{\theta_n + \mathcal{A}^2/2\sigma_{v_n}^2}{\sqrt{\mathcal{A}^2/\sigma_{v_n}^2}}\right), \\ P_{d_n} &= \Pr(\mathcal{P}_{n,t} \neq 0 | h_t = 1) = Q\left(\frac{\theta_n - \mathcal{A}^2/2\sigma_{v_n}^2}{\sqrt{\mathcal{A}^2/\sigma_{v_n}^2}}\right). \end{aligned} \quad (11)$$

Suppose P_{d_n} is required to be fixed at a given value $P_{d_n} = \bar{P}_d, \forall n$. Then the false alarm probability can be written as $P_{f_n} = Q(Q^{-1}(\bar{P}_d) + \sqrt{\mathcal{A}^2/\sigma_{v_n}^2})$. Going back to the transition probability matrix Ψ_n , since the Markov chain characterized by Ψ_n is irreducible and aperiodic, there exists a unique steady state distribution, regardless of the initial state [27]. Let $\Phi_n = [\phi_{n,0}, \phi_{n,1}, \dots, \phi_{n,K}]^T$ be the unique steady state probability vector with the entries $\phi_{n,k} = \lim_{t \rightarrow \infty} \Pr(B_{n,t} = k)$. Note that this vector satisfies the following eigenvalue equation

$$\Phi_n = \Phi_n \Psi_n. \quad (12)$$

In particular, we let Φ_n be the normalized eigenvector of Ψ_n corresponding to the unit eigenvalue, such that the sum of its entries is one [18]. The closed-form expression for Φ_n can be written as [26]

$$\Phi_n = -(\Psi_n^T - \mathbf{I} - \mathbf{B})^{-1} \mathbf{1}, \quad (13)$$

where \mathbf{B} is an all-ones matrix, \mathbf{I} is the identity matrix, and $\mathbf{1}$ is an all-ones column vector. From this point forward, we assume that the battery operates at its steady state and we drop the superscript t .

For clarity of the presentation and to illustrate our transmit power control strategy in (5), we consider the following simple example consisting of one sensor, i.e., $N = 1$, and let $L = 4$, $K = 6$, $\rho = 2$ and $\gamma_{g_1} = 1$. To examine the effect of variations of the scale factors and the quantization thresholds on Ψ_n and Φ_n and transmit power, we consider two sets of values $c_1^{(a)} = [0.1, 0.3, 0.5, 0.7]$, $\mu_1^{(a)} = [0, 0.2, 1.4, 3.6, \infty]$ and $c_1^{(b)} = [0.3, 0.5, 0.7, 0.9]$, $\mu_1^{(b)} = [0, 0.3, 2.5, 4.7, \infty]$. The corresponding 7×7 transition matrices, denoted as $\Psi_1^{(a)}$ and $\Psi_1^{(b)}$, as well as the corresponding 7×1 steady state probability vectors, denoted as $\Phi_1^{(a)}$ and $\Phi_1^{(b)}$ are

⁴A Markov chain is time-homogeneous (stationary) if and only if its transition probability matrix is time-invariant. Adopting homogeneous Markov chain model for studying EH-enabled communication systems is widely common [27].

$$I_{i \rightarrow j}(\mathcal{S}_{n,t}, \mathcal{P}_{n,t} T_s / b_u) = \begin{cases} 1, & \text{if } j = \min \{ [i + \mathcal{S}_{n,t} - \mathcal{P}_{n,t} T_s / b_u]^+, K \}, \\ 0, & \text{o.w.} \end{cases} \quad (8)$$

$$\Psi_1^{(a)} = \begin{pmatrix} 0.13 & 0.27 & 0.27 & 0.17 & 0.09 & 0.03 & 0.04 \\ 0 & 0.13 & 0.27 & 0.27 & 0.18 & 0.09 & 0.06 \\ 0 & 0.02 & 0.15 & 0.27 & 0.25 & 0.16 & 0.15 \\ 0 & 0 & 0.02 & 0.15 & 0.27 & 0.26 & 0.30 \\ 0 & 0 & 0.02 & 0.09 & 0.21 & 0.25 & 0.43 \\ 0 & 0 & 0 & 0.02 & 0.09 & 0.21 & 0.68 \\ 0 & 0 & 0 & 0.02 & 0.04 & 0.09 & 0.85 \end{pmatrix},$$

$$\Psi_1^{(b)} = \begin{pmatrix} 0.14 & 0.28 & 0.28 & 0.16 & 0.07 & 0.04 & 0.03 \\ 0 & 0.14 & 0.28 & 0.28 & 0.16 & 0.09 & 0.05 \\ 0 & 0.06 & 0.19 & 0.27 & 0.22 & 0.13 & 0.13 \\ 0 & 0 & 0.07 & 0.20 & 0.27 & 0.22 & 0.24 \\ 0 & 0 & 0.06 & 0.15 & 0.22 & 0.22 & 0.35 \\ 0 & 0 & 0 & 0.07 & 0.15 & 0.21 & 0.57 \\ 0 & 0 & 0 & 0.07 & 0.12 & 0.14 & 0.67 \end{pmatrix}.$$

$$\Phi_n^{(a)} = [0, 0.0004, 0.0027, 0.0290, 0.0640, 0.1195, 0.7844]$$

$$\Phi_n^{(b)} = [0, 0.0015, 0.0209, 0.1002, 0.1582, 0.1723, 0.5469]$$

Given these two sets of values, Fig. 3 illustrates the two corresponding transmit power maps assuming $b_u = 10$ mJ and $T_s = 10$ sec. The transmit power maps in (5) show how much power the sensor should spend for its data transmission, given its battery state k and the feedback information (i.e., the quantization interval to which the channel gain $g_{1,t}$ belongs). For instance, for the parameters in Fig. (3a), when $g_{1,t} \in \mathcal{I}_{1,2}$ and $B_{1,t} = 3$, then $\mathcal{P}_{1,t} = 1$ mW, whereas for the parameters in Fig. 3b, when $g_{1,t} \in \mathcal{I}_{1,2}$ and $B_{1,t} = 3$, then $\mathcal{P}_{1,t} = 2$ mW.

C. Received Signals at FC and Optimal Bayesian Fusion Rule

In each time slot sensors send their data symbols to the FC over orthogonal fading channels. The received signal at the FC from sensor n corresponding to time slot t is

$$y_{n,t} = g_{n,t} \alpha_{n,t} + w_{n,t}, \quad \text{for } n = 1, \dots, N \quad (14)$$

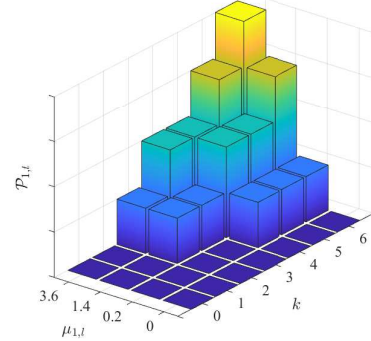
where $w_{n,t} \sim \mathcal{N}(0, \sigma_{w_n}^2)$ is the additive Gaussian noise and $\alpha_{n,t} = \sqrt{\mathcal{P}_{n,t}}$. We assume $w_{n,t}$'s are i.i.d. over time slots and independent across sensors. Let $\mathbf{y}_t = [y_{1,t}, y_{2,t}, \dots, y_{N,t}]$ denote the vector that includes the received signals at the FC from all sensors in time slot t . The FC applies the optimal Bayesian fusion rule $\Gamma_0(\cdot)$ to the received vector \mathbf{y}_t and obtains a global decision $u_{0,t} = \Gamma_0(\mathbf{y}_t)$, where $u_{0,t} \in \{0, 1\}$ [7]. In particular, we have

$$u_{0,t} = \Gamma_0(\mathbf{y}_t) = \begin{cases} 1, & \Delta_t > \tau, \\ 0, & \Delta_t < \tau, \end{cases} \quad (15)$$

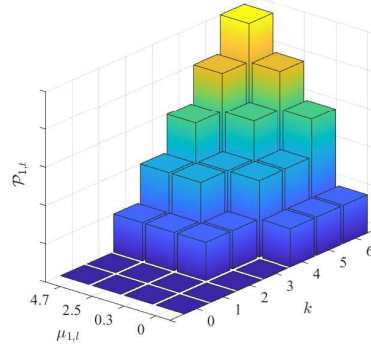
where the decision threshold $\tau = \log(\frac{\Pi_0}{\Pi_1})$ and

$$\Delta_t = \log \left(\frac{f(\mathbf{y}_t | h_t = 1)}{f(\mathbf{y}_t | h_t = 0)} \right), \quad (16)$$

and $f(\mathbf{y}_t | h_t)$ is the conditional probability density function (pdf) of the received vector \mathbf{y}_t at the FC.



(a) $\mu_1^{(a)} = [0, 0.2, 1.4, 3.6]$, $c_1^{(a)} = [0.1, 0.3, 0.5, 0.7]$



(b) $\mu_1^{(b)} = [0, 0.3, 2.5, 4.7]$, $c_1^{(b)} = [0.3, 0.5, 0.7, 0.9]$

Fig. 3: This example shows how much power $\mathcal{P}_{1,t}$ the single sensor should spend for its data transmission, given its battery state and the feedback information.

D. Our Proposed Constrained Optimization Problem

From Bayesian perspective, the natural choice to measure the detection performance corresponding to the global decision $u_{0,t}$ at the FC is the error probability, defined as

$$\begin{aligned} P_e &= \Pi_0 \Pr(u_{0,t} = 1 | h_t = 0) + \Pi_1 \Pr(u_{0,t} = 0 | h_t = 1) \\ &= \Pi_0 \Pr(\Delta_t > \tau | h_t = 0) + \Pi_1 \Pr(\Delta_t < \tau | h_t = 1). \end{aligned} \quad (17)$$

However, finding a closed form expression for P_e is often mathematically intractable. Instead, we choose the total J -divergence between the distributions of the detection statistics at the FC under different hypotheses (will be defined in Section III), as our detection performance metric. This choice allows us to provide a more tractable analysis.

Our goal is to find the scale factors $\{c_{n,l}\}_{l=0}^{L-1}$ and the quantization thresholds $\{\mu_{n,l}\}_{l=1}^{L-1}$ in the transmit power control strategy (5) for all sensors such that the total J -divergence at the FC is maximized, subject to an average transmit power per sensor constraint. We assume that this optimization problem is solved *offline* at the FC, given (i) the statistical information of fading channels and noises (including communication

channel noise and observation noise) and randomly arriving energy units, and (ii) the battery parameter K , the number of quantization levels L , and the given \bar{P}_d for local detectors at the sensors. The solutions to this optimization problem is available *a priori* at the FC and the sensors, to be utilized for controlling and adapting transmit power according to (5). The idea of offline power control optimization with a limited feedback channel has been used before for distributed detection systems in WSNs [14].

III. CHARACTERIZATION OF TOTAL J -DIVERGENCE AND ERROR PROBABILITY

In this section, first we define the total J -divergence and then derive a closed-form expression for it in Section III.A, using Gaussian distribution approximation. Next, considering P_e in (17) we provide a closed-form approximate expression for it in Section III.B, using the same Gaussian distribution approximation and Lindeberg central limit theorem (CLT).

A. Total J -Divergence Derivation

We start with the definition of J -divergence. Consider two pdfs of a continuous random variable x , denoted as $\eta_1(x)$ and $\eta_2(x)$. By definition [9], [13], the J -divergence between $\eta_1(x)$ and $\eta_0(x)$, denoted as $J(\eta_1, \eta_0)$, is

$$J(\eta_1, \eta_0) = D(\eta_1 || \eta_0) + D(\eta_0 || \eta_1), \quad (18)$$

where $D(\eta_i || \eta_j)$ is the non-symmetric Kullback-Leibler (KL) distance between $\eta_i(x)$ and $\eta_j(x)$. The KL distance $D(\eta_i || \eta_j)$ is defined as

$$D(\eta_i || \eta_j) = \int_{-\infty}^{\infty} \log \left(\frac{\eta_i(x)}{\eta_j(x)} \right) \eta_i(x) dx. \quad (19)$$

Substituting (19) into (18) we obtain

$$J(\eta_1, \eta_0) = \int_{-\infty}^{\infty} [\eta_1(x) - \eta_0(x)] \log \left(\frac{\eta_1(x)}{\eta_0(x)} \right) dx. \quad (20)$$

In our problem setup, the two conditional pdfs $f(\mathbf{y}|h=1)$ and $f(\mathbf{y}|h=0)$ play the role of $\eta_1(x)$ and $\eta_0(x)$, respectively. Let J_{tot} denote the J -divergence between $f(\mathbf{y}|h=1)$ and $f(\mathbf{y}|h=0)$. The pdf of vector \mathbf{y} given h is

$$\begin{aligned} f(\mathbf{y}|h) &\stackrel{(a)}{=} \prod_{n=1}^N f(y_n|h) \\ &\stackrel{(b)}{=} \prod_{n=1}^N f(y_n|\alpha_n, h) \Pr(\alpha_n|h) \\ &\stackrel{(c)}{=} \prod_{n=1}^N \underbrace{f(y_n|\alpha_n) \Pr(\alpha_n|h)}_{=f(y_n|h)}, \quad \text{for } h = 0, 1. \end{aligned} \quad (21)$$

Equality (a) in (21) holds since the received signals from sensors at the FC, given h , are conditionally independent, equality (b) in (21) is obtained from Bayes' rule, and equality (c) in (21) is found noting that H , α_n , y_n satisfy the Markov property, i.e., $H \rightarrow \alpha_n \rightarrow y_n$ [9], [13] and hence y_n and H , given α_n , are conditionally independent. Let J_n represent the

J -divergence between the two conditional pdfs $f(y_n|h=1)$ and $f(y_n|h=0)$. Using (20) we can express J_n as

$$J_n = \int_{-\infty}^{\infty} [f(y_n|h=1) - f(y_n|h=0)] \log \left(\frac{f(y_n|h=1)}{f(y_n|h=0)} \right) dy_n. \quad (22)$$

Based on (21) we have $J_{tot} = \sum_{n=1}^N J_n$. To calculate J_n , we need to find the conditional pdf $f(y_n|h)$. Considering (14) we realize that y_n , given α_n , is Gaussian. In particular, we have

$$f(y_n|\alpha_n=0) = \mathcal{N}(0, \sigma_{w_n}^2), f(y_n|\alpha_n \neq 0) = \mathcal{N}(g_n \alpha_n, \sigma_{w_n}^2) \quad (23)$$

Also, considering (11) and noting that $\alpha_n = \sqrt{\bar{P}_n}$ we find

$$\begin{aligned} \Pr(\alpha_n \neq 0|h=0) &= P_{f_n}, \quad \Pr(\alpha_n \neq 0|h=1) = P_{d_n}, \\ \Pr(\alpha_n = 0|h=0) &= 1 - P_{f_n}, \quad \Pr(\alpha_n = 0|h=1) = 1 - P_{d_n}. \end{aligned} \quad (24)$$

Substituting (23) and (24) in (21), the conditional pdfs $f(y_n|h=0)$ and $f(y_n|h=1)$ become

$$\begin{aligned} f(y_n|h=0) &= f(y_n|\alpha_n \neq 0)P_{f_n} + f(y_n|\alpha_n = 0)(1 - P_{f_n}), \\ f(y_n|h=1) &= f(y_n|\alpha_n \neq 0)P_{d_n} + f(y_n|\alpha_n = 0)(1 - P_{d_n}). \end{aligned} \quad (25)$$

Although $f(y_n|\alpha_n=0)$ and $f(y_n|\alpha_n \neq 0)$ in (25) are Gaussian, $f(y_n|h=0)$ and $f(y_n|h=1)$ are Gaussian mixtures, due to P_{d_n} and P_{f_n} . Unfortunately, the J -divergence between two Gaussian mixture densities does not have a general closed-form expression. Similar to [9], [13] we approximate the J -divergence between two Gaussian mixture densities by the J -divergence between two Gaussian densities $f^G(y_n|h) \sim \mathcal{N}(m_{n,h}, \Upsilon_{n,h}^2)$, where the mean $m_{n,h}$ and the variance $\Upsilon_{n,h}^2$ of the approximate distributions are obtained from matching the first and second order moments of the actual and the approximate distributions. For our problem setup, one can verify that the parameters $m_{n,h}$ and $\Upsilon_{n,h}^2$ become

$$\begin{aligned} m_{n,0} &= g_n \alpha_n P_{f_n}, \quad \Upsilon_{n,0}^2 = g_n^2 \alpha_n^2 P_{f_n} (1 - P_{f_n}) + \sigma_{w_n}^2, \\ m_{n,1} &= g_n \alpha_n P_{d_n}, \quad \Upsilon_{n,1}^2 = g_n^2 \alpha_n^2 P_{d_n} (1 - P_{d_n}) + \sigma_{w_n}^2. \end{aligned} \quad (26)$$

The J -divergence between two Gaussian densities, represented as $J(f^G(y_n|h=1), f^G(y_n|h=0))$, in terms of their means and variances is [9]

$$J(f^G(y_n|h=1), f^G(y_n|h=0)) = \frac{\Upsilon_{n,1}^2 + (m_{n,1} - m_{n,0})^2}{\Upsilon_{n,0}^2} + \frac{\Upsilon_{n,0}^2 + (m_{n,0} - m_{n,1})^2}{\Upsilon_{n,1}^2}. \quad (27)$$

Substituting $m_{n,h}$ and $\Upsilon_{n,h}^2$ into J_n in (27) we approximate J_n as the following

$$J_n = \frac{\sigma_{w_n}^2 + A_n g_n^2 \alpha_n^2}{\sigma_{w_n}^2 + B_n g_n^2 \alpha_n^2} + \frac{\sigma_{w_n}^2 + C_n g_n^2 \alpha_n^2}{\sigma_{w_n}^2 + D_n g_n^2 \alpha_n^2}, \quad (28)$$

where

$$\begin{aligned} A_n &= P_{f_n}(1 - P_{d_n}) + P_{d_n}(P_{d_n} - P_{f_n}), \\ C_n &= P_{d_n}(1 - P_{f_n}) - P_{f_n}(P_{d_n} - P_{f_n}), \\ B_n &= P_{d_n}(1 - P_{d_n}), \quad D_n = P_{f_n}(1 - P_{f_n}). \end{aligned}$$

B. Error Probability Approximation

In this section, we provide a closed-form approximate expression for P_e in (17). To find the approximate expression for P_e , we approximate Δ in (16) using a similar Gaussian distribution approximation as we conducted in Section III-A.

In Section III-A we approximated the conditional pdf $f(y_n|h)$ with $f^G(y_n|h) = \mathcal{N}(m_{n,h}, \Upsilon_{n,h}^2)$, where the mean $m_{n,h}$ and the variance $\Upsilon_{n,h}^2$ of the approximate distribution are provided in (26). Relying on this Gaussian distribution approximation, we can also approximate the conditional pdf $f(\mathbf{y}|h)$. In particular, since the received signals at the FC, conditioned on h , are independent across sensors (see (21-a)), we can approximate $f(\mathbf{y}|h)$ with $f^G(\mathbf{y}|h) = \mathcal{N}(\varphi_h, \Lambda_h)$, where φ_h and Λ_h are the mean vector and the *diagonal* covariance matrix with elements $m_{n,h}$ and $\Upsilon_{n,h}^2$, respectively. Using this Gaussian distribution approximation, we can approximate Δ in (16) as

$$\begin{aligned} \Delta &\approx \log \left(\frac{f^G(\mathbf{y}|h=1)}{f^G(\mathbf{y}|h=0)} \right) \\ &= \log \left(\frac{\sqrt{\det \Lambda_0} \exp \left(-\frac{1}{2}(\mathbf{y} - \varphi_1)^T \Lambda_1^{-1} (\mathbf{y} - \varphi_1) \right)}{\sqrt{\det \Lambda_1} \exp \left(-\frac{1}{2}(\mathbf{y} - \varphi_0)^T \Lambda_0^{-1} (\mathbf{y} - \varphi_0) \right)} \right) \\ &= R - \frac{1}{2}(\mathbf{y} - \varphi_1)^T \Lambda_1^{-1} (\mathbf{y} - \varphi_1) + \frac{1}{2}(\mathbf{y} - \varphi_0)^T \Lambda_0^{-1} (\mathbf{y} - \varphi_0), \end{aligned} \quad (29)$$

where $R = \log \left(\frac{\sqrt{\det \Lambda_0}}{\sqrt{\det \Lambda_1}} \right)$. Since the covariance matrices Λ_0 and Λ_1 are diagonal, the approximate expression for Δ in (29) can be rewritten as

$$\begin{aligned} \Delta &\approx R + \frac{1}{2} \Delta'_N, \quad \Delta'_N = \sum_{n=1}^N z_n, \\ z_n &= \frac{(y_n - m_{n,0})^2}{\Upsilon_{n,0}^2} - \frac{(y_n - m_{n,1})^2}{\Upsilon_{n,1}^2}, \end{aligned} \quad (30)$$

With the Gaussian distribution approximation, the optimal fusion rule in (15) can be approximated with

$$u_0 = \begin{cases} 1, & \Delta'_N > \tau', \\ 0, & \Delta'_N < \tau', \end{cases} \quad (31)$$

where Δ'_N is given in (30) and $\tau' = 2(\tau - R)$. The error probability corresponding to the fusion rule in (31) is

$$P_e = \Pi_0 \Pr(\Delta'_N > \tau' | h = 0) + \Pi_1 \Pr(\Delta'_N < \tau' | h = 1). \quad (32)$$

To find P_e in (32) we need the pdf of Δ'_N given h . We note that z_n in (30) can be rewritten as a quadratic function of y_n

$$\begin{aligned} z_n &= ay_n^2 + by_n + c, \quad \text{where} \\ a &= \frac{1}{\Upsilon_{n,0}^2} - \frac{1}{\Upsilon_{n,1}^2}, \quad b = \frac{2m_{n,1}}{\Upsilon_{n,1}^2} - \frac{2m_{n,0}}{\Upsilon_{n,0}^2}, \quad c = \frac{m_{n,0}^2}{\Upsilon_{n,0}^2} - \frac{m_{n,1}^2}{\Upsilon_{n,1}^2}. \end{aligned} \quad (33)$$

Let $\mu_{z_n|h}$ and $\sigma_{z_n|h}^2$ denote the mean and variance of z_n in (33) given h , respectively. To find $\mu_{z_n|h}, \sigma_{z_n|h}^2$ we recall the following fact.

Fact: Let $x \sim \mathcal{N}(\mu, \sigma^2)$ be a Gaussian random variable with the mean $\mathbb{E}\{x\} = \mu$ and the variance $\sigma^2 = \mathbb{E}\{x^2\} - \mu^2$.

Then we have [28]:

$$\begin{aligned} \mathbb{E}\{x^2\} &= \mu^2 + \sigma^2, \\ \mathbb{E}\{x^3\} &= \mu(\mu^2 + 3\sigma^2), \\ \mathbb{E}\{x^4\} &= \mu^4 + 6\mu^2\sigma^2 + 3\sigma^4. \end{aligned} \quad (35)$$

Using this fact, we find

$$\begin{aligned} \mu_{z_n|h} &= a(m_{n,h}^2 + \Upsilon_{n,h}^2) + b m_{n,h} + c, \\ \sigma_{z_n|h}^2 &= 2a^2(2m_{n,h}^2 + \Upsilon_{n,h}^4) + b\Upsilon_{n,h}^2(b + 4a m_{n,h}), \end{aligned} \quad (36)$$

where a, b, c are given in (33) and $m_{n,h}, \Upsilon_{n,h}^2$ are given in (26). Relying on the Gaussian distribution approximation of y_n given h , we can derive the pdf of z_n given h , where the pdf expression is provided in (34). Since given h , z_n 's are independent, the pdf of Δ'_N given h , is convolution of these N individual pdfs, which does not have a closed-form expression. This indicates that, even with the Gaussian distribution approximation, finding a closed-form expression of P_e in (32) for finite N remains *elusive*. Hence, we resort to the *asymptotic regime* when N grows very large and invoke the central limit theorem (CLT) to approximate P_e in (32).

Lindeberg CLT is a variant of CLT, where the random variables are independent, but not necessarily identically distributed [29]. Let $\mu_{\Delta'_N|h}$ and $\sigma_{\Delta'_N|h}^2$ indicate the mean and variance of Δ'_N in (30) given h . We have $\mu_{\Delta'_N|h} = \sum_{n=1}^N \mu_{z_n|h}$ and $\sigma_{\Delta'_N|h}^2 = \sum_{n=1}^N \sigma_{z_n|h}^2$. Assuming Lindeberg's condition, given below, is satisfied

$$\lim_{N \rightarrow \infty} \frac{1}{\sigma_{\Delta'_N|h}^2} \sum_{n=1}^N \mathbb{E}\{(z_n - \mu_{z_n|h})^2\} = 0, \quad (37)$$

then, as N goes to infinity, the normalized sum $(1/\sigma_{\Delta'_N|h}^2) \sum_{n=1}^N (z_n - \mu_{z_n|h})$ converges in distribution toward the standard normal distribution

$$\frac{1}{\sigma_{\Delta'_N|h}^2} \sum_{n=1}^N (z_n - \mu_{z_n|h}) \xrightarrow{d} \mathcal{N}(0, 1), \quad (38)$$

where \xrightarrow{d} indicates convergence in distribution. Using (38) we can approximate P_e in (32) using Q -function

$$P_e = \Pi_0 Q \left(\frac{\tau' - \mu_{\Delta'_N|0}}{\sigma_{\Delta'_N|0}} \right) + \Pi_1 \left[1 - Q \left(\frac{\tau' - \mu_{\Delta'_N|1}}{\sigma_{\Delta'_N|1}} \right) \right]. \quad (39)$$

IV. FORMULATING OUR OPTIMIZATION PROBLEM

As we stated before, our objective is to find the scale factors $\{c_{n,l}\}_{l=0}^{L-1}$ and the quantization thresholds $\{\mu_{n,l}\}_{l=1}^{L-1}$ in the transmit power control strategy (5) for all sensors such that the total J -divergence at the FC is maximized, subject to an average transmit power per sensor constraint. We formulate the optimization problem, via writing the cost function and the constraints in terms of the optimization variables. Recall total J -divergence at the FC is $J_{tot} = \sum_{n=1}^N J_n$, where J_n in given in (28), and transmit power per sensor \mathcal{P}_n is given in (5). We note that J_n depends on g_n value, whereas \mathcal{P}_n depends on the quantization interval to which g_n belongs. The dependency of J_n on g_n stems from the fact that the

$$f(z_n|h) = \frac{1}{g(z_n)} \left\{ f_{y_n|h}^G \left(\frac{\Upsilon_{n,0}^2 \Upsilon_{n,1}^2}{2} g(z_n) + m_{n,0} \Upsilon_{n,1}^2 - m_{n,1} \Upsilon_{n,0}^2 \right) + f_{y_n|h}^G \left(\frac{-\Upsilon_{n,0}^2 \Upsilon_{n,1}^2}{2} g(z_n) + m_{n,0} \Upsilon_{n,1}^2 - m_{n,1} \Upsilon_{n,0}^2 \right) \right\},$$

$$g(z_n) = \frac{2}{\Upsilon_{n,1} \Upsilon_{n,1}} \sqrt{(m_{n,0} - m_{n,1})^2 + z_n (\Upsilon_{n,1}^2 - \Upsilon_{n,0}^2)}. \quad (34)$$

FC has full knowledge of all channel gains g_n 's, and the optimal Bayesian fusion rule utilizes this full information. Hence, the error probability P_e and its bound J_{tot} depend on this full information. On the other hand, sensor n only knows the quantization interval to which g_n belongs, and adapts its transmit power \mathcal{P}_n according to this *partial* knowledge as well as its battery state. We seek the best $\{c_{n,l}\}_{l=0}^{L-1}$ and $\{\mu_{n,l}\}_{l=1}^{L-1}$, such that the solutions we obtain that do not depend on the specific channel gain realizations. Hence, we take the average of J_n and \mathcal{P}_n over g_n , conditioned that $g_n \in [\mu_{n,i}, \mu_{n,i+1})$. By taking such a conditional average over g_n , the solutions we obtain do not depend on the specific channel gain realizations and are valid, as long as the channel gain statistics remain unchanged. The problem can be solved *offline* and its solutions can become available *a priori* at the FC and the sensors. Let $\bar{J}_n^{(i)} = \mathbb{E}\{J_n | g_n \in [\mu_{n,i}, \mu_{n,i+1})\}$ and $\bar{\mathcal{P}}_n^{(i)} = \mathbb{E}\{\mathcal{P}_n | g_n \in [\mu_{n,i}, \mu_{n,i+1})\}$, respectively, denote the expectations of J_n and \mathcal{P}_n over g_n and, conditioned that $g_n \in [\mu_{n,i}, \mu_{n,i+1})$. In the following, we compute the two conditional expectations $\bar{J}_n^{(i)}$ and $\bar{\mathcal{P}}_n^{(i)}$, in terms of the optimization variables. To compute $\bar{J}_n^{(i)}$ we use the following fact.

Fact: Suppose random variable x has an exponential distribution with parameter λ , i.e., the pdf of x is $f(x) = \lambda e^{-\lambda x}$. Consider the function $h(x) = \frac{a+bx}{c+dx}$, with given constants a , b , c and d . Then, the average of $h(x)$, conditioned on x being in the interval $[\mu_i, \mu_{i+1})$ is

$$\begin{aligned} \mathbb{E}\{h(x) | x \in [\mu_i, \mu_{i+1})\} &= \int_{\mu_i}^{\mu_{i+1}} h(x) f(x) dx \\ &= \frac{1}{d} \left[a\beta(\mu_{i+1}) - \frac{bc}{d}\beta(\mu_{i+1}) - be^{-\lambda\mu_{i+1}} \right. \\ &\quad \left. - a\beta(\mu_i) - \frac{bc}{d}\beta(\mu_i) - be^{-\lambda\mu_i} \right], \end{aligned}$$

where

$$\beta(x) = \lambda \exp\left(\frac{c\lambda}{d}\right) \text{Ei}\left(-\lambda x - \frac{c\lambda}{d}\right), \quad \text{Ei}(z) = \int_{-z}^{\infty} \frac{e^{-t}}{t} dt.$$

Using this fact and letting $a_1 = a_2 = c_1 = c_2 = \sigma_{w_n}^2$, $b_1 = A_n \alpha_n^2$, $b_2 = C_n \alpha_n^2$, $d_1 = B_n \alpha_n^2$ and $d_2 = D_n \alpha_n^2$, where A_n, B_n, C_n, D_n are given in (28), we reach at

$$\bar{J}_n^{(i)} = \sum_{k=0}^K \phi_{n,k} \pi_{n,i} \left[\Omega([\underline{c}_{n,i} k], \mu_{n,i+1}^2) - \Omega([\underline{c}_{n,i} k], \mu_{n,i}^2) \right], \quad (40)$$

where the two dimensional function $\Omega(x, y)$ in (40) is

$$\begin{aligned} \Omega(x, y) &\triangleq \\ &\frac{1}{B_n x} \left[\sigma_{w_n}^2 \beta_1(x, y) - \frac{A_n}{B_n} \sigma_{w_n}^2 \beta_1(x, y) - A_n x e^{(-y \gamma_{g_n})} \right] + \\ &\frac{1}{D_n x} \left[\sigma_{w_n}^2 \beta_2(x, y) - \frac{C_n}{D_n} \sigma_{w_n}^2 \beta_2(x, y) - C_n x e^{(-y \gamma_{g_n})} \right], \end{aligned} \quad (41)$$

and the two dimensional functions $\beta_1(x, y)$ and $\beta_2(x, y)$ in (41) are

$$\begin{aligned} \beta_1(x, y) &\triangleq \gamma_{g_n} \exp\left(\frac{\sigma_{w_n}^2 \gamma_{g_n}}{x B_n}\right) \text{Ei}\left(-\gamma_{g_n} y - \frac{\sigma_{w_n}^2 \gamma_{g_n}}{x B_n}\right), \\ \beta_2(x, y) &\triangleq \gamma_{g_n} \exp\left(\frac{\sigma_{w_n}^2 \gamma_{g_n}}{x D_n}\right) \text{Ei}\left(-\gamma_{g_n} y - \frac{\sigma_{w_n}^2 \gamma_{g_n}}{x D_n}\right). \end{aligned}$$

We can compute $\bar{\mathcal{P}}_n^{(i)}$ using (5) as the following

$$\bar{\mathcal{P}}_n^{(i)} = \hat{\Pi}_{n,1} \sum_{k=0}^K \phi_{n,k} \pi_{n,i} [c_{n,i} k] \quad (42)$$

We formulate our problem, denoted as (P1), as the following

$$\begin{aligned} \text{(P1)} \quad &\max_{\{c_{n,l}\}_{l=0}^{L-1}, \{\mu_{n,l}\}_{l=1}^{L-1}, \forall n} \sum_{n=1}^N \sum_{i=0}^{L-1} \bar{J}_n^{(i)} \\ \text{s.t.} \quad &c_{n,l} \in [0, 1], \quad l = 0, \dots, L-1, \forall n \\ &0 < \mu_{n,l} < \infty, \quad l = 1, \dots, L-1, \forall n \\ &\sum_{i=0}^{L-1} \bar{\mathcal{P}}_n^{(i)} \leq \mathcal{P}_0, \quad \forall n \\ &\Phi_n = -(\Psi_n^T - \mathbf{I} - \mathbf{B})^{-1} \mathbf{1}, \quad \forall n \end{aligned}$$

Regarding the implementation of (P1) a remark follows.

Remark: We note that cost function and the constraints in (P1) are *decoupled* across sensors. Hence, (P1) can be decomposed into n sub-problems, denoted as (P2), as the following

$$\begin{aligned} \text{(P2)} \quad &\max_{\{c_{n,l}\}_{l=0}^{L-1}, \{\mu_{n,l}\}_{l=1}^{L-1}} \sum_{i=0}^{L-1} \bar{J}_n^{(i)} \\ \text{s.t.} \quad &c_{n,l} \in [0, 1], \quad l = 0, \dots, L-1, \\ &0 < \mu_{n,l} < \infty, \quad l = 1, \dots, L-1, \\ &\sum_{i=0}^{L-1} \bar{\mathcal{P}}_n^{(i)} \leq \mathcal{P}_0, \\ &\Phi_n = -(\Psi_n^T - \mathbf{I} - \mathbf{B})^{-1} \mathbf{1}. \end{aligned}$$

This implies that solving (P1) is equivalent to solving (P2) N times for $n = 1, \dots, N$. It also implies that solving (P1)

can lend itself to a *distributed* implementation, where sensor n solves its corresponding (P2) independent of the other sensors. For implementing our proposed power control strategy, we assume that the FC solves (P1) once. Based on the obtained solution, in each time slot t the FC quantizes $g_{n,t}$'s and informs sensor n of the quantization interval to which $g_{n,t}$ belongs, via a limited feedback channel. Sensor n solves its corresponding (P2) once, and based on the obtained solution it sets its transmit power control strategy in (5) once. Then, in each time slot t sensor n chooses its transmit power $P_{n,t}$ according to (5), considering its battery state and the received feedback information. It is worth mentioning the difference between optimizing the total J -divergence and the approximate P_e expression in (39). Different from (P1), the approximate P_e expression in (39) *cannot be decoupled* across sensors. Therefore, constrained minimization of P_e does not render itself to a distributed implementation, i.e. each sensor needs to solve (P1), with P_e in (39) being the cost function, which ensues a much higher computational complexity.

V. SOLVING PROBLEM (P1)

Since solving (P1) is equivalent to solving (P2) N times, in this section we focus on solving (P2). Let examine how the cost function and the constraints in (P2) depend on the optimization variables.

- Dependency of $\bar{J}_n^{(i)}$: Considering (40), its explicit dependency on $\{c_{n,l}, \mu_{n,l}\}$'s is clear. It also depends implicitly on $\{c_{n,l}, \mu_{n,l}\}$'s through the probabilities $\pi_{n,l}$'s and the vector entries $\phi_{n,k}$'s. Recall that $\phi_{n,k}$'s are the entries of vector Φ_n given in (13). This vector depends on the matrix Ψ_n , whose entries are given in (9) and depend on $\{c_{n,l}, \mu_{n,l}\}$'s.

- Dependency of $\bar{P}_n^{(i)}$: Considering (42), its explicit dependency on $c_{n,l}$'s is clear. It also depends implicitly on $\{c_{n,l}, \mu_{n,l}\}$'s through $\pi_{n,l}$'s and $\phi_{n,k}$'s.

- Dependency of Φ_n : It depends implicitly on $\{c_{n,l}, \mu_{n,l}\}$'s. We note that problem (P2) is *not concave* with respect to the optimization variables. Moreover, the objective function and the constraints in (P2) are *not differentiable* with respect to the optimization variables. Hence, existing gradient-based algorithms for solving non-convex optimization problems cannot be used to solve (P2).

A. Deterministic Search Method

We resort to a grid-based search method, which requires $(2L - 1)$ -dimensional search over the search (parameter) space $[0, 1]^L \times (0, \infty)^{L-1}$. To curb the computational complexity of this grid-based search, we can limit $\mu_{n,l}$'s to a maximum value, denoted as μ_{max} . We refer to the solution obtained from solving (P2) using this method the *optimal* solution, in the sense that it is the *best* attainable solution for (P2). Clearly, the accuracy of this solution depends on the resolution of the grid-based search. Suppose the intervals $[0, 1]$ and $(0, \mu_{max}]$ are divided into N_c and N_μ sub-intervals, respectively. Therefore, the search space of (P2), denoted as \mathcal{D} , consists of $(N_c)^L (N_\mu)^{L-1}$ discrete points in the original $(2L - 1)$ -dimensional search space. To find the computational complexity of obtaining the *optimal* solution

for (P2), we note that the solver unit (either FC or sensor n) needs to perform two tasks for each point in \mathcal{D} : task (i) forming Ψ_n and solving (13) to find Φ_n , task (ii) calculating $\bar{J}_n^{(i)}$ and $\bar{P}_n^{(i)}$. Our numerical results show that for a fixed $\{c_{n,l}\}_{l=0}^{L-1}$ and $\{\mu_{n,l}\}_{l=1}^{L-1}$ the computational complexity of task (i) and task (ii) are $\mathcal{O}(K^{3.2})$ and $\mathcal{O}(K^{1.1})$, respectively. Hence, the computational complexity of finding the *optimal* solution for (P2) is $\mathcal{O}(N_c^L N_\mu^{L-1} (K^{3.2} + K^{1.1}))$. Since $K^{1.1}$ order is dominated by $K^{3.2}$, the computational complexity of finding the *optimal* solution for (P2) can be simplified to $\mathcal{O}(N_c^L N_\mu^{L-1} K^{3.2})$.

B. Random Search Method

Finding the *optimal* solution of (P2) using the grid-based search, as described above, requires searching search space \mathcal{D} *deterministically*. In contrast, in a *random* search algorithm, only a randomly chosen subset of the points in \mathcal{D} is searched to find a solution. The size of this subset can be chosen to be smaller than $(N_c)^L (N_\mu)^{L-1}$, and hence, the computational complexity of finding a solution using a random search algorithm can be significantly lowered. We refer to the solution obtained from solving (P2) using a random search algorithm the *c-optimal* solution, in the sense that it is a close-to-optimal solution.

Among the random search algorithms in the literature, we choose the so-called “Recursive Random Search (RRS) algorithm” [30]. Our reason for this choice is that the authors in [30] showed that RRS algorithm outperforms significantly the traditional search algorithms (e.g., genetic algorithms, multi-start hill climbing algorithms, and simulated annealing algorithm) for most optimization problems. RRS algorithm consists of two phases: exploration (global) phase and exploitation (local) phase. In exploration phase, the algorithm performs random sampling from the entire sample space \mathcal{D} , to inspect the overall form of the objective function, and to identify “promising areas” in \mathcal{D} [30]. In exploitation phase, the algorithm continues to search *only* within the identified “promising areas”, using recursive random sampling. As the search continues, the sample space is shrunk gradually (according to the previously drawn samples), and the algorithm learns more details of the objective function, until it finally converges to a local optimum, which will be considered as the solution of the optimization problem in hand [30]. For our work to be self-contained, in the following we overview RRS algorithm, with reference to the lines in the pseudo-code of Algorithm 1.

- *Exploration Phase*: To describe this phase and to illustrate the efficiency of RRS algorithm in finding the solution of (P2), we need to first introduce the following notations and concepts. Suppose $x = [c_{n,0}, \dots, c_{n,L-1}, \mu_{n,1}, \dots, \mu_{n,L-1}]$ denote a sample (point) in \mathcal{D} , and J_{min}, J_{max} indicate the minimum and the maximum values of the objective function, respectively. We define the distribution function of the objective function values as $r = \frac{m(A_{\mathcal{D}}(r))}{m(\mathcal{D})}$, for $r \in [0, 1]$, where $m(\cdot)$ denotes the cardinality of the set. Given r value, set $A_{\mathcal{D}}(r) \subset \mathcal{D}$ with the cardinality $m(A_{\mathcal{D}}(r)) = r \times m(\mathcal{D})$ is the set of points in

\mathcal{D} whose values of the objective function exceed a threshold $J_{tr} \in [J_{min}, J_{max}]$.

$$A_{\mathcal{D}}(r) = \left\{ x \in \mathcal{D} \mid \sum_{i=0}^{L-1} \bar{J}_n^{(i)}(x) \geq J_{tr}(r) \right\}, m(A_{\mathcal{D}}(r)) = r \times m(\mathcal{D})$$

For this reason $A_{\mathcal{D}}(r)$ is called the r -percentile set in \mathcal{D} [30]. We note that $A_{\mathcal{D}}(1) = \mathcal{D}$ and $\lim_{r \rightarrow 0} A_{\mathcal{D}}(r)$ converges to the global optimum of the problem [30]. Now, consider the r -percentile set $A_{\mathcal{D}}(r)$ in \mathcal{D} and its corresponding $J_{tr}(r)$ value. The goal in exploration phase is to reach a point in $A_{\mathcal{D}}(r)$ with probability p , via random sampling. The question is: how many random samples of \mathcal{D} should we draw, such that we reach a point in $A_{\mathcal{D}}(r)$ with probability p ?

To answer this question, let $\mathbf{X} = \{x_j\}_{j=1}^{Q_1}$ be the set of randomly drawn samples from \mathcal{D} that satisfy the average transmit power constraint in (P2), and $x_j^* \in \mathbf{X}$ provides the largest value of the objective function. We have

$$p = \Pr(x_j^* \in A_{\mathcal{D}}(r)) = 1 - \Pr(x_j^* \notin A_{\mathcal{D}}(r)) = 1 - (1-r)^{Q_1}.$$

Solving p for r we reach at $r = 1 - (1-p)^{1/Q_1}$. Solving p for Q_1 we obtain $Q_1 = \frac{\ln(1-p)}{\ln(1-r)}$. For any probability value p , as Q_1 increases, r tends to 0 and $\lim_{r \rightarrow 0} A_{\mathcal{D}}(r)$ converges to the global maximum of (P2).

Lines 2,3,4 of the pseudo-code correspond to this phase. We take Q_1 random samples from \mathcal{D} , each denoted as x_{q_1} , and put them in $\mathbf{X}_t = \{x_{q_1}\}_{q_1=1}^{Q_1}$ and initialize $\mathbf{X} = \{\}$. For each sample $x_{q_1} \in \mathbf{X}_t$, we check whether the average transmit power constraint is held. If the constraint is satisfied, x_{q_1} is added to \mathbf{X} . If the constraint is not satisfied, we take another sample from the set $\mathcal{D} \setminus \mathbf{X}_t$ and add this new sample to \mathbf{X}_t . We repeat this procedure until $m(\mathbf{X})$ reaches Q_1 . Using the samples in $\mathbf{X} = \{x_j\}_{j=1}^{Q_1}$, the algorithm computes the threshold J_{tr} . Having the set \mathbf{X} , whose elements represent the ‘‘promising areas’’ in \mathcal{D} , the algorithm enters exploitation phase. Any future sample we encounter in the next phase that has a greater value of the objective function than J_{tr} belongs to $A_{\mathcal{D}}(r)$.

• *Exploitation Phase:* Consider $\mathbf{X} = \{x_j\}_{j=1}^{Q_1}$. For each sample $x_j \in \mathbf{X}$ we first determine several neighborhoods⁵ $N_{\rho}(x_j)$ for $\rho = 1, \dots, \rho_0$, such that $m(N_{\rho}(x_j)) < m(N_{\rho+1}(x_j))$. Given the parameter⁶ Q_2 , the description of the recursive random search in these neighborhoods to find the solution of (P2) follows.

For each sample $x_j \in \mathbf{X}$, we start by letting the search space be $\mathcal{S} = N_{\rho_0}(x_j)$, and search \mathcal{S} hoping to find a *better* sample than x_j . In particular, we take Q_2 random samples from $N_{\rho_0}(x_j)$, each denoted as x_{q_2} , and put them in $\mathbf{Y}_t = \{x_{q_2}\}_{q_2=1}^{Q_2}$ and initialize $\mathbf{Y}_j = \{\}$. For each sample $x_{q_2} \in \mathbf{Y}_t$, we check two conditions: (i) whether the average transmit power constraint is held, (ii) whether the objective

function evaluated at x_{q_2} provides a larger value than J_{tr} . If both constraints are satisfied, x_{q_2} is added to \mathbf{Y}_j . After checking all samples in \mathbf{Y}_t we examine \mathbf{Y}_j . Depending on whether $\mathbf{Y}_j \neq \{\}$, meaning there exists at *least one better* sample than x_j in \mathcal{S} , or $\mathbf{Y}_j = \{\}$, meaning *no better* sample than x_j is found in \mathcal{S} , we take two different actions.

If $\mathbf{Y}_j \neq \{\}$ we select the sample in \mathbf{Y}_j that provides the largest value of the objective function, denoted as x_i^* , and replace $x_j \in \mathbf{X}$ with x_i^* , and change \mathcal{S} from $N_{\rho_0}(x_j)$ to $N_{\rho_0}(x_i^*)$, and continue with searching the new \mathcal{S} . This procedure of changing the center of \mathcal{S} (without shrinking it) in exploitation phase is called ‘‘re-align sub-phase’’ [30]. However, if $\mathbf{Y}_j = \{\}$ we shrink \mathcal{S} by changing \mathcal{S} to $N_{\rho_0-1}(x_j)$. This procedure of shrinking \mathcal{S} (without changing its center) in exploitation phase is called ‘‘shrink sub-phase’’ [30]. When searching $N_{\rho_0-1}(x_j)$, if we find a *better* sample than x_j , we replace $x_j \in \mathbf{X}$ with this *better* sample. Otherwise, we further shrink \mathcal{S} by changing \mathcal{S} to $N_{\rho_0-2}(x_j)$. We alternatively perform re-align and shrink sub-phases for x_j , until we get to search the smallest neighborhood $N_1(\cdot)$ of a sample. Note that we limit the number of times we perform re-align sub-phase during the exploitation procedure for x_j to Q_1 , relying on the fact that after drawing Q_1 samples from \mathcal{D} we reach a point in $A_{\mathcal{D}}(r)$ with probability p . At this point, the exploitation procedure for x_j ends, and $x_j \in \mathbf{X}$ is either *kept unchanged* or *replaced with a better sample* that is found during its exploitation procedure. We repeat the exploitation procedure for all samples in \mathbf{X} , and at the end we obtain a refined and fully exploited \mathbf{X} . We let the solution of (P2) be $\arg \max_{x_j \in \mathbf{X}} (\sum_{i=0}^{L-1} \bar{J}_n^{(i)}(x_j))$.

To find the computational complexity of obtaining the c -optimal solution for (P2), we note that during the exploitation phase the solver unit needs to perform *repeatedly* the same two tasks, task (i) and task (ii) in Section V-A, with computational complexity $\mathcal{O}(K^{3.2})$ and $\mathcal{O}(K^{1.1})$, respectively. To find out the number of repetition of tasks, we focus on the exploitation procedure for $x_j \in \mathbf{X}$. After each performance of re-aligning \mathcal{S} or shrinking \mathcal{S} , we randomly search \mathcal{S} . i.e., we evaluate the objective function Q_2 times. Hence, the number of repetition of tasks for each $x_j \in \mathbf{X}$ is equal to $Q_2 \times \#(\text{performing re-align}) \times \#(\text{performing shrink})$. Since $\#(\text{performing re-align}) \leq Q_1$ and $\#(\text{performing shrink}) \leq \rho_0$, the computational complexity corresponding to the exploitation procedure for $x_j \in \mathbf{X}$ is upper bounded by $\mathcal{O}(Q_2 Q_1 \rho_0 (K^{3.2} + K^{1.1}))$. Therefore, the computational complexity of finding the c -optimal solution for (P2) is upper bounded by $\mathcal{O}(Q_2 Q_1^2 \rho_0 (K^{3.2} + K^{1.1}))$, which can be simplified to $\mathcal{O}(Q_2 Q_1^2 \rho_0 K^{3.2})$.

C. Hybrid Deterministic-Random Search Method

In this section we propose a *hybrid* method to find the optimization variable $\{c_{n,l}, \mu_{n,l}\}$'s. In particular, we first obtain the quantization thresholds $\{\mu_{n,l}\}$'s using a different objective function. Then given the optimized $\{\mu_{n,l}\}$'s, we solve (P3),

⁵The neighborhood $N_{\rho}(x_j)$, for $\rho = 1, \dots, \rho_0$, is the set of samples that are neighbors of x_j . Its size $m(N_{\rho}(x_j))$ depends on the dimensionality of search space \mathcal{D} ($(2L-1)$ here) and the resolution of the grid (parameters N_c, N_{μ} here). To identify different neighborhoods of x_j , we have used MATLAB's function *neighbourND*. For instance, for $L=2$ and $N_c=10, N_{\mu}=100$ we have $m(N_1(x_j))=17, m(N_2(x_j))=60, m(N_3(x_j))=139$.

⁶To enable efficient random search even in the smallest neighborhood we choose $Q_2 < m(N_1(\cdot))$.

Algorithm 1: pseudo-code of RSS algorithm

```

1: Initialization phase:
   • Set parameter space  $\mathcal{D}$  with  $(N_c)^L \times (N_\mu)^{L-1}$  points;
   • Initialize exploration parameters  $(p, r)$  and let  $Q_1 = \ln(1-p)/\ln(1-r)$ ;
   • Initialize exploitation parameter  $Q_2$  based on  $(N_c, N_\mu, L)$ ;
2: Start exploration phase, take  $Q_1$  uniform random samples from  $\mathcal{D}$  and put them in  $\mathbf{X}_t = \{x_{q_1}\}_{q_1=1}^{Q_1}$ , initialize  $\mathbf{X} = \{\}$ ;
3: repeat
   for  $x_{q_1} \in \mathbf{X}_t$  do
     if  $\sum_{i=0}^{L-1} \bar{\mathcal{P}}_n^{(i)}(x_{q_1}) \leq \mathcal{P}_0$  then
       Put  $x_{q_1}$  in  $\mathbf{X}$ ;
     else
       Take another sample from  $\mathcal{D} \setminus \mathbf{X}_t$  and add it to  $\mathbf{X}_t$ ;
     end
   end
until  $m(\mathbf{X}) = Q_1$ ;
4: Calculate the threshold using the samples in  $\mathbf{X} = \{x_j\}_{j=1}^{Q_1}$ ,  $J_{tr} = 1/Q_1 \sum_{j=1}^{Q_1} \left( \sum_{i=0}^{L-1} \bar{J}_n^{(i)}(x_j) \right)$ ;
5: Start exploitation phase, determine the neighborhoods of sample  $x_j$  as  $N_1(x_j), N_2(x_j), \dots, N_{\rho_0}(x_j)$ ;
for  $x_j \in \mathbf{X}$  do
  Initialize  $\mathbf{Y}_j = \{\}$ ,  $I = 0$ , Take  $Q_2$  uniform random samples from  $N_\rho(x_j)$  and put them in  $\mathbf{Y}_t = \{x_{q_2}\}_{q_2=1}^{Q_2}$ ;
  for  $x_{q_2} \in \mathbf{Y}_t$  do
    if  $\sum_{i=0}^{L-1} \bar{J}_n^{(i)}(x_{q_2}) \geq J_{tr}$  &  $\sum_{i=0}^{L-1} \bar{\mathcal{P}}_n^{(i)}(x_{q_2}) \leq \mathcal{P}_0$  then
      Add  $x_{q_2}$  to  $\mathbf{Y}_j$ ;
    end
  end
  if  $\mathbf{Y}_j \neq \{\}$  &  $I < Q_1$  then
     $x_i^* = \arg \max_{x_i \in \mathbf{Y}_j} \left( \sum_{i=0}^{L-1} \bar{J}_n^{(i)}(x_i) \right)$ , replace  $x_j \in \mathbf{X}$  with  $x_i^*$ , change the search space from  $N_\rho(x_j)$  to  $N_\rho(x_i^*)$ ;
     $I = I + 1$ ;
  else
    change the search space from  $N_\rho(x_j)$  to  $N_{\rho-1}(x_j)$ ;
  end
end
6:  $x_{opt} = \arg \max_{x_j \in \mathbf{X}} \left( \sum_{i=0}^{L-1} \bar{J}_n^{(i)}(x_j) \right)$ ;

```

given below, using RSS algorithm.

$$\begin{aligned}
\text{(P3)} \quad & \max_{\{c_{n,l}\}_{l=0}^{L-1}} \sum_{i=0}^{L-1} \bar{J}_n^{(i)} \\
\text{s.t. } & c_{n,l} \in [0, 1], \quad l = 0, \dots, L-1, \\
& \sum_{i=0}^L \bar{\mathcal{P}}_n^{(i)} \leq \mathcal{P}_0, \\
& \Phi_n = -(\Psi_n^T - \mathbf{I} - \mathbf{B})^{-1} \mathbf{1}.
\end{aligned}$$

We refer to the solution we obtain using this hybrid method the *sub-optimal* solution, in the sense that it is worse than the *optimal* solution. The *sub-optimal* solution is also worse than *c-optimal* solution for two reasons: (i) we detangle optimizing $\{\mu_{n,l}\}$'s and $\{c_{n,l}\}$'s, (ii) we use a different objective function to optimize $\{\mu_{n,l}\}$'s. The main advantage of using this hybrid method is that finding the *sub-optimal* solution has a lower computational complexity than that of the *c-optimal* solution. Our numerical results in Section VI show that the objective

function values at the *c-optimal* and the *sub-optimal* solutions are very close to each other and also very close to that of the *optimal* solution. In the following, we consider two different objective functions that we use to obtain the optimal $\{\mu_{n,l}\}$'s. To motivate these objective functions, we consider the input-output relationship of the quantizer in Section II-B $\bar{g}_n = Q(g_n)$. If the quantizer input g_n lies in the interval $\mathcal{I}_{n,l}$ then the quantizer output is $\bar{g}_n = \mu_{n,l}$. The quantization error is $e_n = g_n - \bar{g}_n$.

1) *Finding $\{\mu_{n,l}\}$'s via Minimizing Mean Absolute Error (MMAE):* The first objective function we consider is mean of absolute quantization error (MAE), denoted as $\mathbb{E}\{|g_n - \bar{g}_n|\}$. We can express MAE as follows.

$$\mathbb{E}\{|g_n - \bar{g}_n|\} = \sum_{l=0}^{L-1} \int_{\mu_{n,l}}^{\mu_{n,l+1}} (x - \mu_{n,l}) f_{g_n}(x) dx \quad (43)$$

To find $\{\mu_{n,l}\}$'s that minimize MAE, we take the first derivative of MAE with respect to $\mu_{n,l}$ and set the derivative equal to zero. We reach at

$$F_{g_n}(\mu_{n,l+1}) = F_{g_n}(\mu_{n,l}) + (\mu_{n,l} - \mu_{n,l-1}) f_{g_n}(\mu_{n,l}) \quad (44)$$

Recall $\mu_{n,0} = 0$ and $\mu_{n,L} = \infty$, and hence $F_{g_n}(0) = 0$ and $F_{g_n}(\infty) = 1$. We initiate $\mu_{n,1}$ and find $\mu_{n,2}$ using (44). Having $\mu_{n,1}, \mu_{n,2}$, we find $\mu_{n,3}$ using (44). We repeat this until we find all $\{\mu_{n,l}\}$'s. At this point, we check whether the condition $F_{g_n}(\infty) = 1$ is met. If $F_{g_n}(\infty)$ is less (greater) than one, we increase (decrease) the initial value of $\mu_{n,1}$ and find a new set of values for $\{\mu_{n,l}\}$'s. We continue changing the initial value of $\mu_{n,1}$ and finding new values for $\{\mu_{n,l}\}$'s, until the condition $F_{g_n}(\infty) = 1$ is satisfied.

2) *Finding $\{\mu_{n,l}\}$'s via Maximizing output Entropy (MOE):* The second objective function we consider is the mutual information between g_n and \bar{g}_n , denoted as $I(g_n; \bar{g}_n)$. We have $I(g_n; \bar{g}_n) = H(\bar{g}_n) - H(\bar{g}_n|g_n)$, where $H(x)$ denotes the entropy of discrete random variable x . To find $\{\mu_{n,l}\}$'s that maximize $I(g_n; \bar{g}_n)$, we note that $H(\bar{g}_n|g_n)$ is zero, since $\bar{g}_n = Q(g_n)$ and hence, given g_n , \bar{g}_n is also known. Furthermore, $H(\bar{g}_n)$ is maximized when \bar{g}_n follows a uniform distribution, i.e., we set $\pi_{n,l} = \Pr(\mu_{n,l} \leq g_n < \mu_{n,l+1}) = \frac{1}{L+1}$. and the threshold $\mu_{n,l}$ can be obtained as $\mu_{n,l} = \gamma_{g_n} \ln \left(1 - \frac{l}{L+1} \right)$.

The computational complexity of finding the *sub-optimal* solution for (P2) is the sum of two terms. The first term is the computational complexity of finding $\{c_{n,l}\}$'s using RRS algorithm in Section V-B, and is upper bounded by $\mathcal{O}(Q_2 Q_1^2 \rho_0 (K^{3.2} + K^{1.1}))$. We note that Q_2 in this section is chosen according to $m(N_1(\cdot))$, which depends on (L, N_c) , whereas Q_2 in Section V-B is chosen according to $m(N_1(\cdot))$, which depends⁷ on (L, N_c, N_μ) . Hence, Q_2 here is smaller than Q_2 in Section V-B. The second term is the computational complexity of finding $\{\mu_{n,l}\}$'s optimizing one of the two objective functions in this section. The computational complexity of finding $\{\mu_{n,l}\}$'s via MMAE is negligible, due to the simplicity of solving (44). Our simulations show that for different L values, solving (44) takes only several msec.

⁷For instance, for $L=2$ and $N_c=10, N_\mu=100$, we choose $Q_2 < 17$ in Section V-B and we choose $Q_2 < 5$ here.

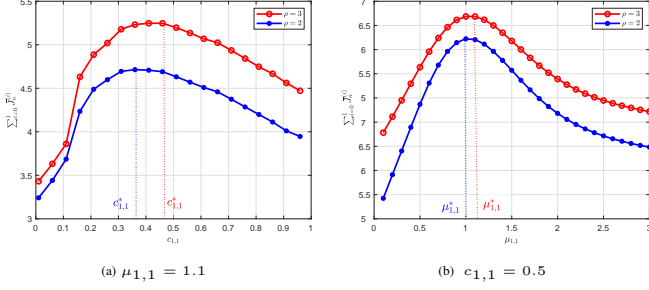


Fig. 4: $K = 5$, $c_{1,0} = 0.3$, $\gamma_{g_1} = 1$.

		$\Pr(B_1 = 0)$	$\Pr(B_1 = 50)$	\bar{B}_1
(a)	$\mu_{1,l} = [0, 0.8, 1.2, \infty]$ $c_{1,l} = [0.3, 0.4, 0.2]$	≈ 0	0.0451	31.97
(b)	$\mu_{1,l} = [0, 0.8, 1.2, \infty]$ $c_{1,l} = [0.5, 0.7, 0.9]$	0.0318	0.0023	14.33
(c)	$\mu_{1,l} = [0, 0.1, 2, \infty]$ $c_{1,l} = [0.4, 0.6, 0.3]$	0.0265	0.0039	15.32
(d)	$\mu_{1,l} = [0, 0.01, 0.1, \infty]$ $c_{1,l} = [0.4, 0.6, 0.3]$	≈ 0	0.0357	28.32

TABLE I: The values of $\Pr(B_1 = 0)$, $\Pr(B_1 = 50)$, \bar{B}_1 for $K = 50$, $\rho = 10$, $\gamma_{g_1} = 1$.

The computational complexity of finding $\{\mu_{n,l}\}$'s via MOE is almost zero, due to the available closed-form solutions.

VI. SIMULATION RESULTS AND DISCUSSION

We corroborate our analysis with MATLAB simulations and investigate: (i) the effect of the optimization variables on the objective function and the entries of Φ in (12), (ii) the accuracy of different search methods in Section V in solving (P2) as well as the existing trade-off between detection performance and average transmit power, (iii) the behavior of the optimized scale factors $\{c_l\}$'s with respect to the fading channel gain g_n , (iv) the accuracy of the P_e approximate in (39). (v) the dependency of the system error probability P_e (achieved with the optimized variables) on K, ρ, L , and the SNR corresponding to observation channel defined as $\text{SNR}_s = 20 \log(\mathcal{A}/\sigma_v)$.

• **Effect of optimization variables:** Considering one sensor and $L = 2$, the optimization variables are $\{c_{1,0}, c_{1,1}, \mu_{1,1}\}$. Fig. 4a illustrates the objective function $\sum_{i=0}^{L-1} \bar{J}_1^{(i)}$ versus the scale factor $c_{1,1}$. We observe that the objective function is not a concave function of $c_{1,1}$. Still there exists a point, denoted as $c_{1,1}^*$, at which the function attains its maximum. Starting from small values of $c_{1,1}$, as $c_{1,1}$ increases (until it reaches $c_{1,1}^*$), the function value increases, because the harvested energy can recharge the battery and can yield more power for data transmission. However, when $c_{1,1}$ exceeds $c_{1,1}^*$, the harvested and stored energy cannot support the data transmission and the function value decreases. Fig. 4b shows the objective function versus the quantization threshold $\mu_{1,1}$. We observe that the objective function is not a concave function of $\mu_{1,1}$. Still there exists a point, denoted as $\mu_{1,1}^*$, at which the function achieves its maximum.

To accentuate the effect of the optimization variables on the entries of Φ we define the average energy stored at the battery of sensor n as $\bar{B}_n = \mathbb{E}\{B_n\} = \sum_{k=0}^K k \phi_{n,k}$,

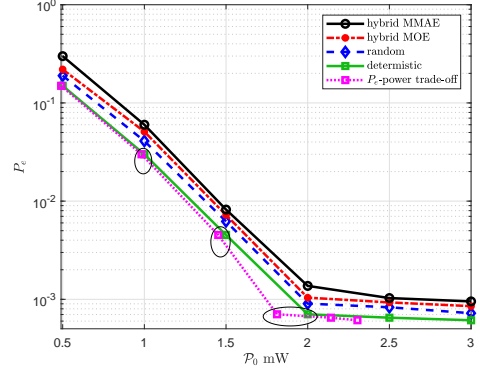


Fig. 5: P_e vs. \mathcal{P}_0 for $N = 3$, $K = 5$, $L = 2$, $\rho = 2$, $\sigma_{w_n}^2 = 1$, $\gamma_{g_n} = 2$, $P_{d_n} = 0.9$, $\forall n$, $\text{SNR}_s = 3\text{dB}$.

where the largest possible value for \bar{B}_n is K . Table I shows $\Pr(B_1 = 0)$, $\Pr(B_1 = 50)$, \bar{B}_1 for four choices (a), (b), (c), (d). Going from (a) to (b), we note that given μ_l 's, as c_l 's increase data transmit power in (5) increases. Due to large energy consumption for data transmission \bar{B}_1 decreases and the chance of energy outage increases. Going from (c) to (d), we note that given c_l 's, as μ_l 's decrease, $\Pr(B_1 = 50)$ increases and $\Pr(B_1 = 0)$ decreases, and \bar{B}_1 increases. Due to small energy consumption for data transmission, the chance of having near full battery increases, indicating that sensor has failed to utilize the excess energy. Both energy outage and energy overflow inevitably impact transmission and detection performance, leading to a reduction in the objective function.

• **Accuracy of different search methods in solving (P2) and detection performance-transmit power trade-off:** First, we compare the accuracy of deterministic, random, and hybrid search methods in Section V in solving (P2). Fig. 5 shows P_e versus \mathcal{P}_0 for $L = 2$. To plot the curve labeled as “deterministic” first we obtain the *optimal* solution, set transmit power control strategy in (5) accordingly, and run Monte-Carlo simulation to find P_e . Similarly, we plot the curves labeled as “random”, “hybrid MMAE”, “hybrid MOE” using the *c-optimal* solution, the *sub-optimal* solution corresponding to MMAE, and the *sub-optimal* solution corresponding to MOE, respectively. When using RRS algorithm we choose the parameters of exploration phase $p = 0.99$, $r = 0.1$, leading to $Q_1 = 44$. For exploitation phase, we choose $Q_2 = 10$ for “random” and $Q_2 = 3$ for “hybrid MMAE” and “hybrid MOE”. Note that for all curves, as \mathcal{P}_0 increases P_e decreases, which is expected. Also, “random”, “hybrid MMAE” and “hybrid MOE” perform very close to “deterministic”. Fig. 5 also allows us to examine the existing trade-off between the average transmit power and the detection performance. Consider the curve labeled “ P_e -power trade-off” in Fig. 5, which shows how much average transmit power is required to provide a certain P_e value. This curve is obtained from examining the points on “deterministic” and checking whether the power constraint in (P2) is active or inactive. At a given point, when this constraint is active (inactive), the average transmit power is equal to (less than) \mathcal{P}_0 . Note that as \mathcal{P}_0 increases and P_e reaches an error floor, the average transmit power is less than \mathcal{P}_0 .

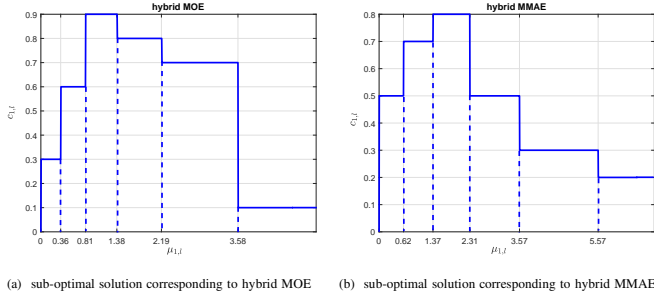


Fig. 6: $K = 5$, $L = 6$, $\rho = 2$, $\sigma_{w_1}^2 = 1$, $\gamma_{g_1} = 2$, $P_{d_1} = 0.9$, $\mathcal{P}_0 = 2\text{mW}$, $\text{SNR}_s = 2\text{ dB}$.

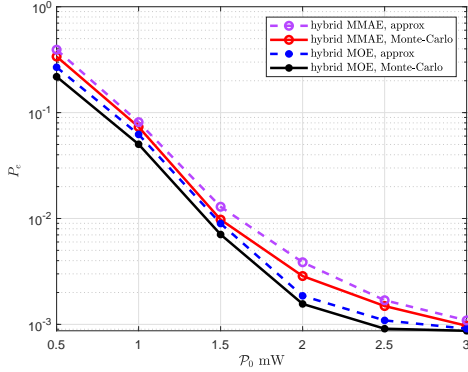


Fig. 7: P_e vs. \mathcal{P}_0 for $N = 5$, $K = 5$, $L = 3$, $\rho = 2$, $\sigma_{w_n}^2 = 1$, $\gamma_{g_n} = 2$, $P_{d_n} = 0.9$, $\forall n$, $\text{SNR}_s = 3\text{ dB}$.

Since finding the *sub-optimal* solution has the lowest computational complexity, and its performance is very close to the *optimal* solution, from this point forward, we focus on “hybrid MMAE” and “hybrid MOE”.

- **Behavior of the optimized scale factors:** Considering one sensor and $L = 6$, the optimization variables are $\{c_{1,l}\}_{l=0}^5, \{\mu_{1,l}\}_{l=1}^5$. Fig. 6a and Fig. 6b depict the optimized $\{c_{1,l}, \mu_{1,l}\}$'s corresponding to “hybrid MMAE” and “hybrid MOE”. We note that, as l increases (i.e., channel gain $g_{n,t}$ increases), the length of quantization interval $(\mu_{1,l+1} - \mu_{1,l})$ becomes larger. Also, $c_{1,l}$ first increases and then decreases. Considering (5) this implies that, given the battery state k , as $g_{n,t}$ increases $\mathcal{P}_{n,t}$ first increases and then decreases.

- **Accuracy of P_e approximate in (39):** To examine the accuracy of P_e approximate in (39), we focus on “hybrid MMAE” and “hybrid MOE”. Fig. 7 plots P_e versus \mathcal{P}_0 , in which P_e values obtained from Monte-Carlo simulations are denoted as “Monte-Carlo”, and P_e values obtained from (39) are denoted as “approx”. This figure suggests that the P_e approximate in (39) is reasonably accurate. Henceforth, from this point forward, we use (39) to plot P_e .

- **Dependency of P_e on different parameters:** Fig. 8-10 plot P_e corresponding to “hybrid MMAE” and “hybrid MOE” in terms of different system parameters. Fig. 8 depicts P_e versus K as γ_{g_n} changes. As K increases P_e decreases, until it reaches an error floor. This is because for large K , power $\mathcal{P}_{n,t}$ in (5) is no longer restricted by K , and instead it is restricted by ρ . Also, the communication channel noise $\sigma_{w_n}^2$ becomes dominant and leads to an error floor. Clearly,

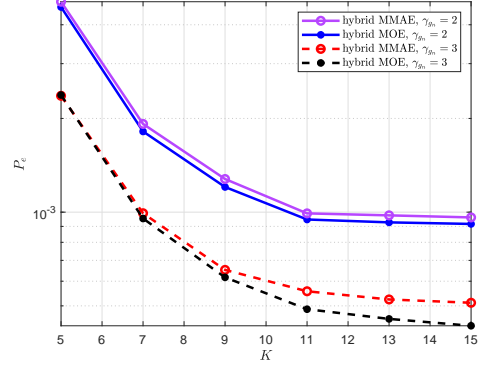


Fig. 8: P_e vs. K for $N = 5$, $L = 3$, $\rho = 5$, $\sigma_{w_n}^2 = 1$, $P_{d_n} = 0.9$, $\forall n$, $\mathcal{P}_0 = 3\text{mW}$, $\text{SNR}_s = 5\text{ dB}$.

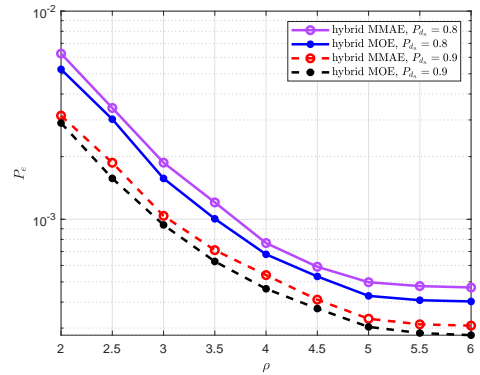


Fig. 9: P_e vs. ρ for $N = 5$, $K = 5$, $L = 3$, $\sigma_{w_n}^2 = 1$, $\gamma_{g_n} = 3$, $\forall n$, $\mathcal{P}_0 = 3\text{mW}$, $\text{SNR}_s = 3\text{ dB}$.

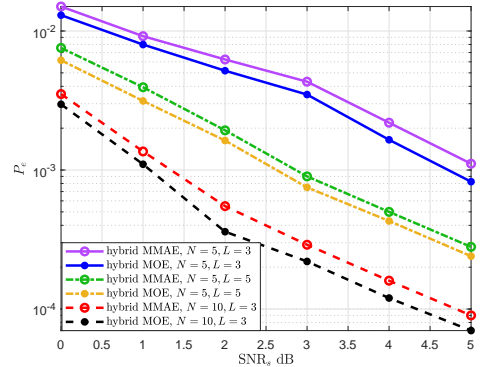


Fig. 10: P_e vs. SNR_s for $K = 5$, $\rho = 2$, $\sigma_{w_n}^2 = 1$, $\gamma_{g_n} = 2$, $P_{d_n} = 0.9$, $\forall n$, $\mathcal{P}_0 = 2\text{mW}$.

the error floor becomes smaller when γ_{g_n} increases. Also, “hybrid MOE” outperforms “hybrid MMAE”. Fig. 9 shows P_e versus ρ as \bar{P}_d changes. As ρ increases P_e decreases, until it reaches an error floor. This is because for large ρ , power $\mathcal{P}_{n,t}$ is no longer limited by the amount of harvested energy. Instead, $\sigma_{w_n}^2$ becomes the dominant factor and leads to an error floor. Also, increasing \bar{P}_d lowers the error floor. Fig. 10 shows P_e versus SNR_s as N, L vary. Given N, L as SNR_s increases, P_e decreases. Increasing N and L reduce P_e . Also, as L increases, the gap between “hybrid MMAE” and “hybrid

MOE” decreases.

VII. CONCLUSIONS

We developed a power control strategy for an EH-enabled WSN, that is tasked with solving a binary distributed detection problem. Our proposed strategy is parametrized in terms of the channel gain quantization thresholds and the scale factors, which play key roles in balancing the rates of energy harvesting and energy consumption for transmission. We explored the optimal and sub-optimal strategies such that the J -divergence based detection metric is maximized, subject to an average transmit power per sensor constraint. These optimization problems can be solved offline and allow each sensor to adapt its power based on its battery state and its quantized CSI (acquired via limited feedback from the FC). Since our non-convex optimization problem is not differentiable with respect to the optimization variables, we explored deterministic, random, and hybrid grid-based search methods, and showed that our proposed hybrid search methods have a low-computational complexity and near-optimal performance. The structure of the optimized scale factors reveals that, given the battery state, the optimized power level is not a monotonic function of the channel gain. We examined the existing trade-off between the average transmit power and the detection performance. We also demonstrated that increasing K or ρ do not necessarily lower the detection error, and it depends on the communication channel noise.

REFERENCES

- [1] G. Ardeshiri, H. Yazdani, and A. Vosoughi, “Optimal local thresholds for distributed detection in energy harvesting wireless sensor networks,” in *2018 IEEE Global Conference on Signal and Information Processing (GlobalSIP)*, Nov 2018, pp. 813–817.
- [2] G. Ardeshiri, H. Yazdani, and A. Vosoughi, “Power adaptation for distributed detection in energy harvesting wsns with finite-capacity battery,” in *2019 IEEE Global Communications Conference (GLOBECOM)*. IEEE, 2019, pp. 1–6.
- [3] M.-L. Ku, W. Li, Y. Chen, and K. R. Liu, “Advances in energy harvesting communications: Past, present, and future challenges,” *IEEE Communications Surveys & Tutorials*, vol. 18, no. 2, pp. 1384–1412, 2015.
- [4] R. R. Tenney and N. R. Sandell, “Detection with distributed sensors,” *IEEE Transactions on Aerospace and Electronic systems*, no. 4, pp. 501–510, 1981.
- [5] I. Y. Hoballah and P. K. Varshney, “Distributed bayesian signal detection,” *IEEE Transactions on Information Theory*, vol. 35, no. 5, pp. 995–1000, 1989.
- [6] B. Chen, L. Tong, and P. K. Varshney, “Channel-aware distributed detection in wireless sensor networks,” *IEEE Signal Processing Magazine*, vol. 23, no. 4, pp. 16–26, 2006.
- [7] H. R. Ahmadi and A. Vosoughi, “Distributed detection with adaptive topology and nonideal communication channels,” *IEEE transactions on signal processing*, vol. 59, no. 6, pp. 2857–2874, 2011.
- [8] N. Maleki and A. Vosoughi, “On bandwidth constrained distributed detection of a known signal in correlated gaussian noise,” *IEEE Transactions on Vehicular Technology*, 2020.
- [9] X. Zhang, H. V. Poor, and M. Chiang, “Optimal power allocation for distributed detection over MIMO channels in wireless sensor networks,” *IEEE Transactions on Signal Processing*, vol. 56, no. 9, pp. 4124–4140, Sep. 2008.
- [10] H.-s. Kim and N. A. Goodman, “Power control strategy for distributed multiple-hypothesis detection,” *IEEE Transactions on Signal Processing*, vol. 58, no. 7, pp. 3751–3764, 2010.
- [11] H. R. Ahmadi and A. Vosoughi, “Impact of channel estimation error on decentralized detection in bandwidth constrained wireless sensor networks,” in *MILCOM 2008-2008 IEEE Military Communications Conference*. IEEE, 2008, pp. 1–7.
- [12] —, “Channel aware sensor selection in distributed detection systems,” in *2009 IEEE 10th Workshop on Signal Processing Advances in Wireless Communications*. IEEE, 2009, pp. 71–75.
- [13] Z. Hajibabaei, A. Vosoughi, and N. Mastrorarde, “Optimal power allocation for M-ary distributed detection in the presence of channel uncertainty,” *Signal Processing*, vol. 169, p. 107400, 2020.
- [14] X. Guo, Y. He, S. Atapattu, S. Dey, and J. S. Evans, “Power allocation for distributed detection systems in wireless sensor networks with limited fusion center feedback,” *IEEE Transactions on Communications*, vol. 66, no. 10, pp. 4753–4766, Oct 2018.
- [15] A. G. Marques, X. Wang, and G. B. Giannakis, “Minimizing transmit-power for coherent communications in wireless sensor networks using quantized channel state information,” in *2007 IEEE International Conference on Acoustics, Speech and Signal Processing-ICASSP’07*, vol. 3. IEEE, 2007, pp. III–529.
- [16] M. K. Banavar, C. Tepedelenlioglu, and A. Spanias, “Estimation over fading channels with limited feedback using distributed sensing,” *IEEE Transactions on Signal Processing*, vol. 58, no. 1, pp. 414–425, 2009.
- [17] M. Fanaei, M. C. Valenti, and N. A. Schmid, “Limited-feedback-based channel-aware power allocation for linear distributed estimation,” in *2013 Asilomar Conference on Signals, Systems and Computers*. IEEE, 2013, pp. 547–551.
- [18] A. Tarighati, J. Gross, and J. Jaldén, “Decentralized hypothesis testing in energy harvesting wireless sensor networks,” *IEEE Transactions on Signal Processing*, vol. 65, no. 18, pp. 4862–4873, Sep. 2017.
- [19] J. Geng and L. Lai, “Non-bayesian quickest change detection with stochastic sample right constraints,” *IEEE Transactions on Signal Processing*, vol. 61, no. 20, pp. 5090–5102, 2013.
- [20] S. S. Gupta, S. K. Pallapothu, and N. B. Mehta, “Ordered transmissions for energy-efficient detection in energy harvesting wireless sensor networks,” *IEEE Transactions on Communications*, vol. 68, no. 4, pp. 2525–2537, 2020.
- [21] T. Li, P. Fan, and K. B. Letaief, “Outage probability of energy harvesting relay-aided cooperative networks over rayleigh fading channel,” *IEEE Transactions on Vehicular Technology*, vol. 65, no. 2, pp. 972–978, 2015.
- [22] Z. Wang, V. Aggarwal, and X. Wang, “Iterative dynamic water-filling for fading multiple-access channels with energy harvesting,” *IEEE Journal on Selected Areas in Communications*, vol. 33, no. 3, pp. 382–395, 2015.
- [23] M. Nourian, S. Dey, and A. Ahlén, “Distortion minimization in multi-sensor estimation with energy harvesting,” *IEEE Journal on Selected Areas in Communications*, vol. 33, no. 3, pp. 524–539, 2015.
- [24] H. Liu, G. Liu, Y. Liu, L. Mo, and H. Chen, “Adaptive quantization for distributed estimation in energy-harvesting wireless sensor networks: a game-theoretic approach,” *International Journal of Distributed Sensor Networks*, vol. 10, no. 7, p. 217918, 2014.
- [25] A. Taherpour, H. Mokhtarzadeh, and T. Khattab, “Optimized error probability for weighted collaborative spectrum sensing in time-and energy-limited cognitive radio networks,” *IEEE Transactions on Vehicular Technology*, vol. 66, no. 10, pp. 9035–9049, 2017.
- [26] H. Yazdani and A. Vosoughi, “Steady-state rate-optimal power adaptation in energy harvesting opportunistic cognitive radios with spectrum sensing and channel estimation errors,” *IEEE Transactions on Green Communications and Networking*, 2021.
- [27] J. F. Shortle, J. M. Thompson, D. Gross, and C. M. Harris, *Fundamentals of queueing theory*. John Wiley & Sons, 2018, vol. 399.
- [28] A. Winkelbauer, “Moments and absolute moments of the normal distribution,” *arXiv preprint arXiv:1209.4340*, 2012.
- [29] W. Lindeberg, “Eine neue herleitung des exponentialgesetzes in der wahrscheinlichkeitsrechnung,” *Mathematische Zeitschrift*, vol. 15, no. 1, pp. 211–225, 1922.
- [30] T. Ye and S. Kalyanaraman, “A recursive random search algorithm for large-scale network parameter configuration,” in *Proceedings of the 2003 ACM SIGMETRICS International conference on Measurement and modeling of computer systems*, 2003, pp. 196–205.